AD-A269 838

Technical Report GL-93-20
August 1993

2

US Army Corps
of Engineers
Waterways Experiment
Station

Effects of Variable Tire Pressure on Road Surfacings

Volume II: Analysis of Test Results

by *Donald M. Smith*
Geotechnical Laboratory

Prepared for U.S. Department of Agriculture Forest Service

Technical Report GL-93-20
August 1993

Effects of Variable Tire Pressure on Road Surfacings

Volume II: Analysis of Test Results

by Donald M. Smith
Geotechnical Laboratory

U.S. Army Corps of Engineers
Waterways Experiment Station
3909 Halls Ferry Road
Vicksburg, MS 39180-6199

Final report

Prepared for U.S. Department of Agriculture Forest Service
Technology and Development Center
444 East Bonita Avenue
San Dimas, CA 91773

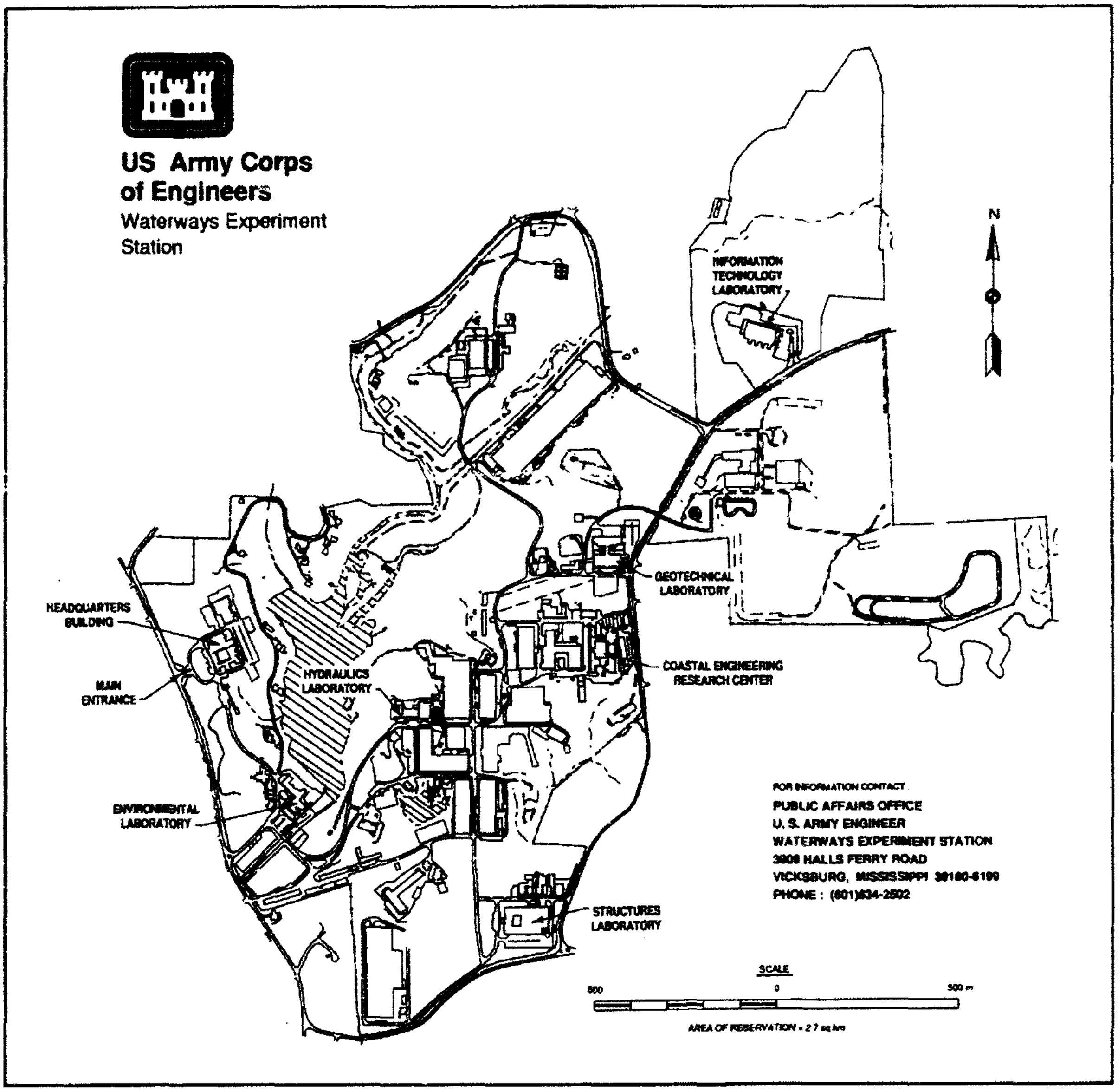

Waterways Experiment Station Cataloging-in-Publication Data

Smith, Donald M.
Effects of variable tire pressure on road surfacings. Volume II, Analysis of test results / by Donald M. Smith ; prepared for U.S. Department of Agriculture Forest Service, Technology and Development Center.
84 p. : ill. ; 28 cm. -- (Technical report ; GL-93-20 v. 2)
Includes bibliographical references.
1. Pavements, Asphalt concrete -- Testing. 2. Automobiles -- Tires -- Inflation pressure -- Environmental aspects. 3. Roads, Gravel -- Testing. 4. Pavements -- Testing. I. Technology & Development Center (San Dimas, Calif.) II. U.S. Army Engineer Waterways Experiment Station. III. Title. IV. Series: Technical report (U.S. Army Engineer Waterways Experiment Station) ; GL-93-20 v. 2.
TA7 W34 no.GL-93-20 v.2

Contents

List of Figures

List of Tables

Preface

The authority for this study is contained in a Technical Support Agreement to construct and operate a low-speed, low-volume test road at the U.S. Army Engineer Waterways Experiment Station (WES). This agreement between the U.S. Department of Agriculture Forest Service, Technology and Development Center (TDC), San Dimas, CA, and WES, Vicksburg, MS, is dated 22 August 1986. This agreement was amended on 18 September 1990. In the agreement it was agreed that WES would document, reduce, and analyze the data gathered during the operation of the test road. This action was completed September 1992. Reduction and documentation of data are treated in Volume I of this report, and this volume describes the analysis of the data.

This analysis was performed at WES, Geotechnical Laboratory (GL), under the general supervision of Drs. William F. Marcuson III, Director, GL, and George M. Hammitt II, Chief, Pavement Systems Division (PSD), GL. Direct supervision was provided by Mr. Jim W. Hall, Chief, Systems Analysis Branch, PSD. The analysis and report preparation were performed by Mr. Donald M. Smith, PSD. The author acknowledges Messrs. P. S. McCaffrey, Jr., C. R. Gonzalez, R. W. Grau, S. L. Webster, D. M. Ladd, and Dr. W. R. Barker, PSD, for their assistance during this analysis.

At the time of publication of this report, Director of WES was Dr. Robert W. Whalin. Commander was COL Bruce K. Howard, EN.

Conversion Factors, Non-SI to SI Units of Measurement

Non-SI units of measurement used in this report can be converted to SI units as follows:

Multiply	By	To Obtain
feet	0.3048	meters
inches	2.54	centimeters
kips (force)	4.448222	kilonewtons
miles (U.S. statute)	1.609347	kilometers
pounds (force)	4.448222	newtons
pounds (force) per square inch	6.894757	kilopascals
pounds (mass)	0.4535924	kilograms
square feet	0.09290304	square meters
square inches	6.4516	square centimeters

1 Introduction

Background

Construction of a low-volume test road was completed in September 1988 at the U.S. Army Engineer Waterways Experiment Station (WES) in support of a research program for the U.S. Department of Agriculture Forest Service (USFS). The research program was performed to assess the effects of reduced tire pressure on road surfacing as it pertained to central tire inflation systems (CTI) that allowed the driver to adjust a vehicle's tire pressure while in motion. The traffic tests were completed with instrumented log trucks on the test road in November 1989. Based on the recommendations in the original report documenting the performance of the test road under traffic (Grau 1990), an additional analytical effort was authorized to summarize all measurements and adapt or develop design models which would account for the behavior of the road surfacings under variable tire pressures.

Objective

The objectives of this report were to provide an analytical summary of the types of test results obtained from the traffic applied to the test road and to use those test results to analyze, adapt, and develop design models which account for variable tire pressures on low-volume aggregate surfaced and asphalt concrete (AC) surfaced roads.

Scope

The report covering this study was divided into two volumes. Volume I (Grau 1992) covered Design, Construction, and Behavior under Traffic. Volume II covers Analysis of Test Results. A brief summary of the test results and observed surface deterioration are included in this volume. The summary provided for the development and analysis of design models incorporating variable tire pressures. The analysis addressed existing design models and compared the proposed models to measured results. A means for

addressing the performance of different subgrade and aggregate types was also included in the design models and predictions.

Review of Previous Work

A number of design methods have been developed with applicability toward the design and analysis of low volume loads. These design methods can be divided into two basic philosophies: (1) mechanistic procedures which utilize the basic concepts of engineering mechanics to characterize pavement behavior under traffic and (2) empirical/statistical procedures which rely on observation and measurement of actual pavement performance and statistical formulations to characterize pavement behavior under traffic. In this analysis the majority of the effort was placed on updating the empirical relationships currently used by the forest service (FS) for designing pavements and characterizing pavement performance. In order to understand the complex interaction of pavement systems with vehicle loads, a limited mechanistic analysis was performed on the AC surfaced items of the test road. The following is a summary of the origins of the currently used FS design equations and their development.

The majority of design methods for aggregate- and earth-surfaced roads found in the literature are generally related to each other and can normally be traced back to two common points of origin. In these models tire pressure is accounted for in mainly two ways: (1) as a variable directly required in a set of input parameters, (2) determined from wheel load and contact area by mathematical computation, or assumed as a constant. The first study is the California Bearing Ratio (CBR) design method, developed by the California Division of Highways for flexible pavements and adapted to airfield design by the U.S. Army Corps of Engineers prior to World War II. The second study is the American Association of State Highway and Transportation Officials (AASHTO) road test. The CBR-based procedures account for more variables and design parameters due to the number of fixed parameters used in the AASHTO road test (ARE, Inc. Engineering Consultants 1989).

The CBR equation was originally presented (Porter 1938, 1942) as the following empirical relationship:

$$t = k\sqrt{(P)} \tag{1}$$

where

t = pavement thickness, in.[1]

---

[1] A table of factors for converting non-SI units of measurement to SI units is presented on page viii.

P = wheel load, lb

k = a constant for a particular CBR and tire pressure

The basic equation was modified by the U.S. Army Corps of Engineers through a continuing process in order to better adapt the procedure to airfield pavement design requirements. These adaptations resulted in the full CBR equation:

$$t = (0.23 Log C + 0.15)\sqrt{\frac{P}{8.1CBR} - \frac{A_c}{\pi}} \tag{2}$$

where

C = coverages of a single wheel

CBR = CBR of the subgrade, percent

A_c = contact area of a single wheel, sq in.

By 1961 the Corps revised road and street design criteria (Brown and Ahlvin 1961) provided a relationship between equivalent operations factors (in terms of an 18-kip equivalent single-axle loads) and design thickness. This provided a means for combining the effects of an array of vehicle loadings into a single magnitude of an 18-kip single-axle equivalents (Ahlvin 1991). In 1971 a new CBR equation was developed as a result of the multiple-wheel-heavy-gear load tests (Hammitt et al. 1971). This equation, although different in form, provides the same results as Equation 2 with extended capabilities in the range of higher levels of load. The newer equation is presented below:

$$\frac{T}{\sqrt{A_c}} = \alpha_i \left[-0.0481 - 1.1562 \left[\log \frac{CBR}{P} \right] - 0.6414 \left[\log \frac{CBR}{P} \right]^2 - 0.4370 \left[\log \frac{CBR}{P} \right]^3 \right] \tag{3a}$$

$$\alpha_i = [0.23 \log(c) + 0.15] \tag{3b}$$

where

T = pavement thickness, in.

A_c = tire contact area, sq in.

α_i = load repetition factor

CBR = CBR of the subgrade material

P = ESWL or SW tire contact pressure, psi

ESWL = equivalent single-wheel load, lb

Equation 3 formed the basis of a portion of the analysis performed on the asphalt-surfaced CTI test items.

The AASHTO road test provided a large amount of data on pavement design and performance. The 1986 AASHTO guide for design of pavement structures incorporated this data into design guidance for both high-volume and low-volume roads. The design procedures presented in the AASHTO guide are primarily aimed at nomograph based solutions to highway design. The low-volume aggregate surfaced road design charts are strictly chart-based solutions with no provisions for an alternative equation-based solution. The basic charts used in this type of design are shown in Figures 1 and 2. Because of this inherent inflexibility the AASHTO aggregate-surfaced design procedure will not be used in the analysis of the data from the CTI test road. The AASHTO flexible pavement design procedure can be used in an equation-based or chart-based form. A discussion of the parameters in the equation will be presented in Chapter 3. The nomograph is based on the AASHTO flexible pavement design equation as shown below, and the design nomographs are shown in Figure 3 (AASHTO 1986).

$$Log_{10}W_{18} = R(S_o) + 9.36\,Log_{10}(SN + 1) - 0.20 + \left[\frac{Log_{10}\left[\frac{\Delta PSI}{4.2 - 1.5}\right]}{0.4 + \left[\frac{1094}{(SN + 1)^{5.19}}\right]}\right] + 2.32\,Log_{10}M_R - 8.07 \tag{4}$$

$$SN = a_1D_1 + a_2D_2 + a_3D_3 \tag{5}$$

where

W_{18} = traffic in 18-kip equivalent single-axle loads

R = reliability factor, percent

S_o = standard deviation of traffic and performance prediction

SN = structural number of pavement

ΔPSI = change in present serviceability index due to W_{18}

M_R = resilient modulus of the subgrade, psi

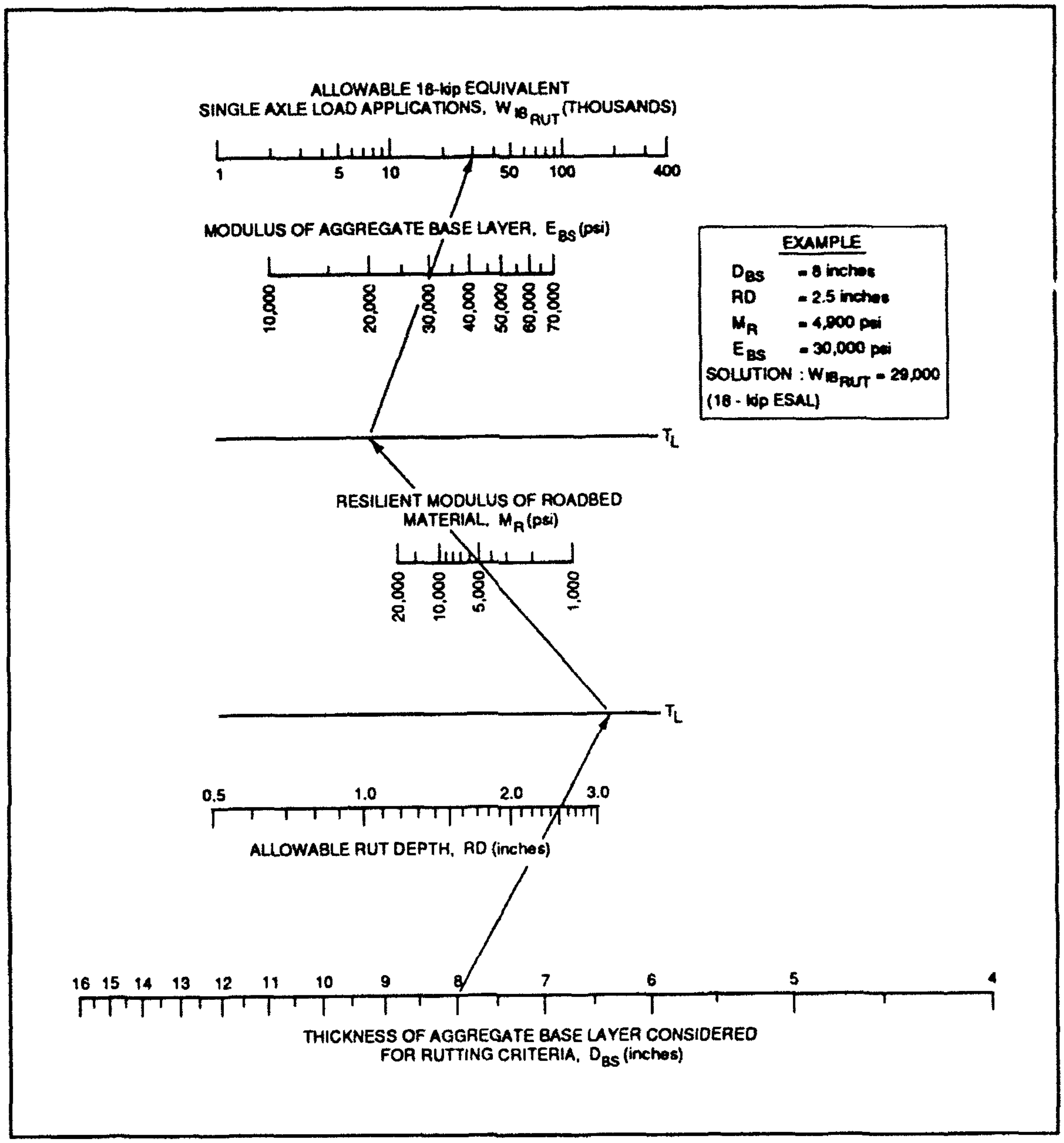

Figure 1. Design chart for aggregate-surfaced roads considering allowable rutting

a_i = i[th] layer coefficient

D_i = i[th] layer thickness, in.

Equations 3 to 5 and their related charts provide the basis for using the Corps flexible pavement design procedure and the AASHTO flexible pavement design procedure as the empirically based tools for analyzing the data from the CTI AC-surfaced test items.

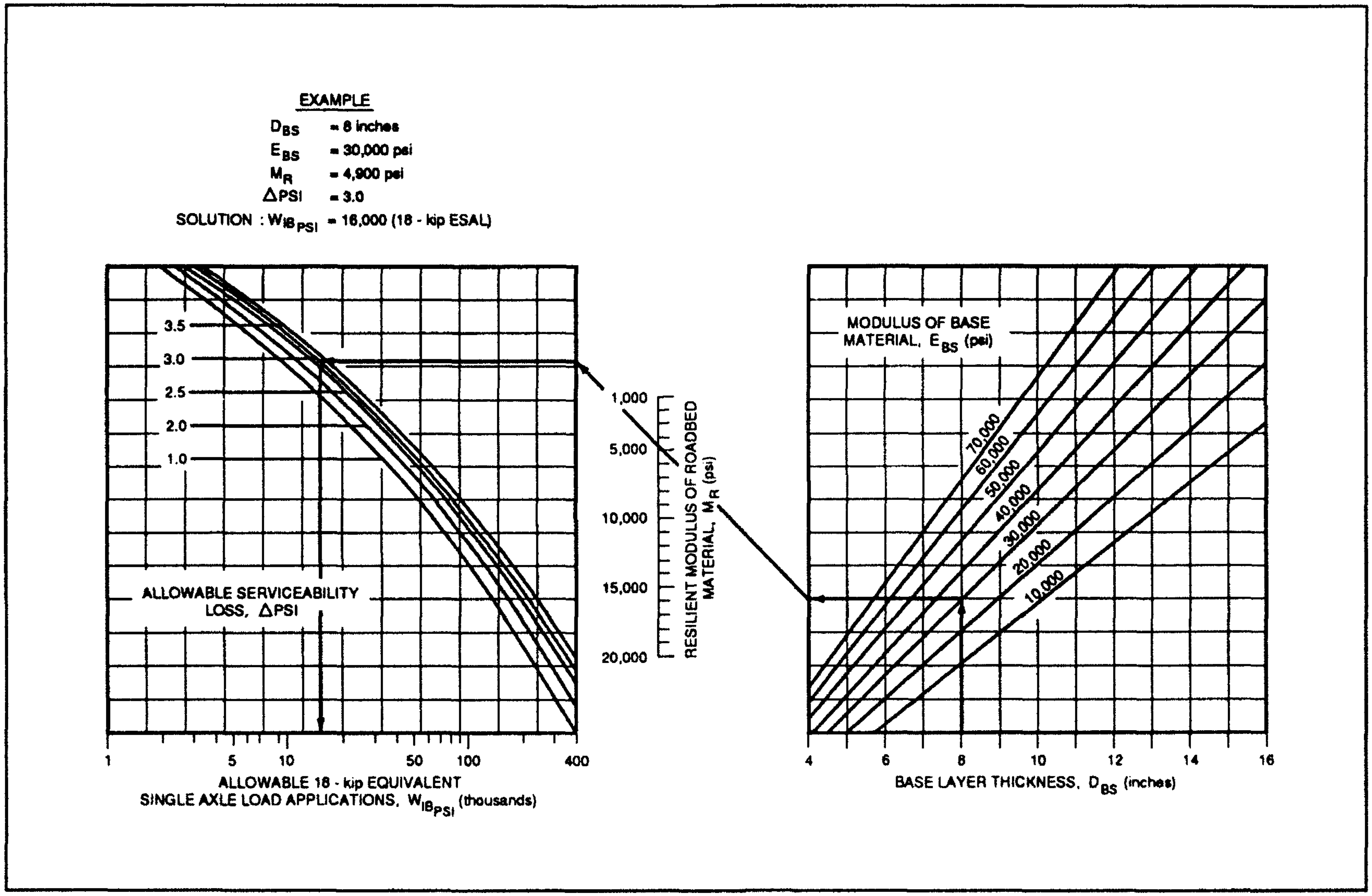

Figure 2. Design chart for aggregate-surfaced roads considering allowable serviceability loss

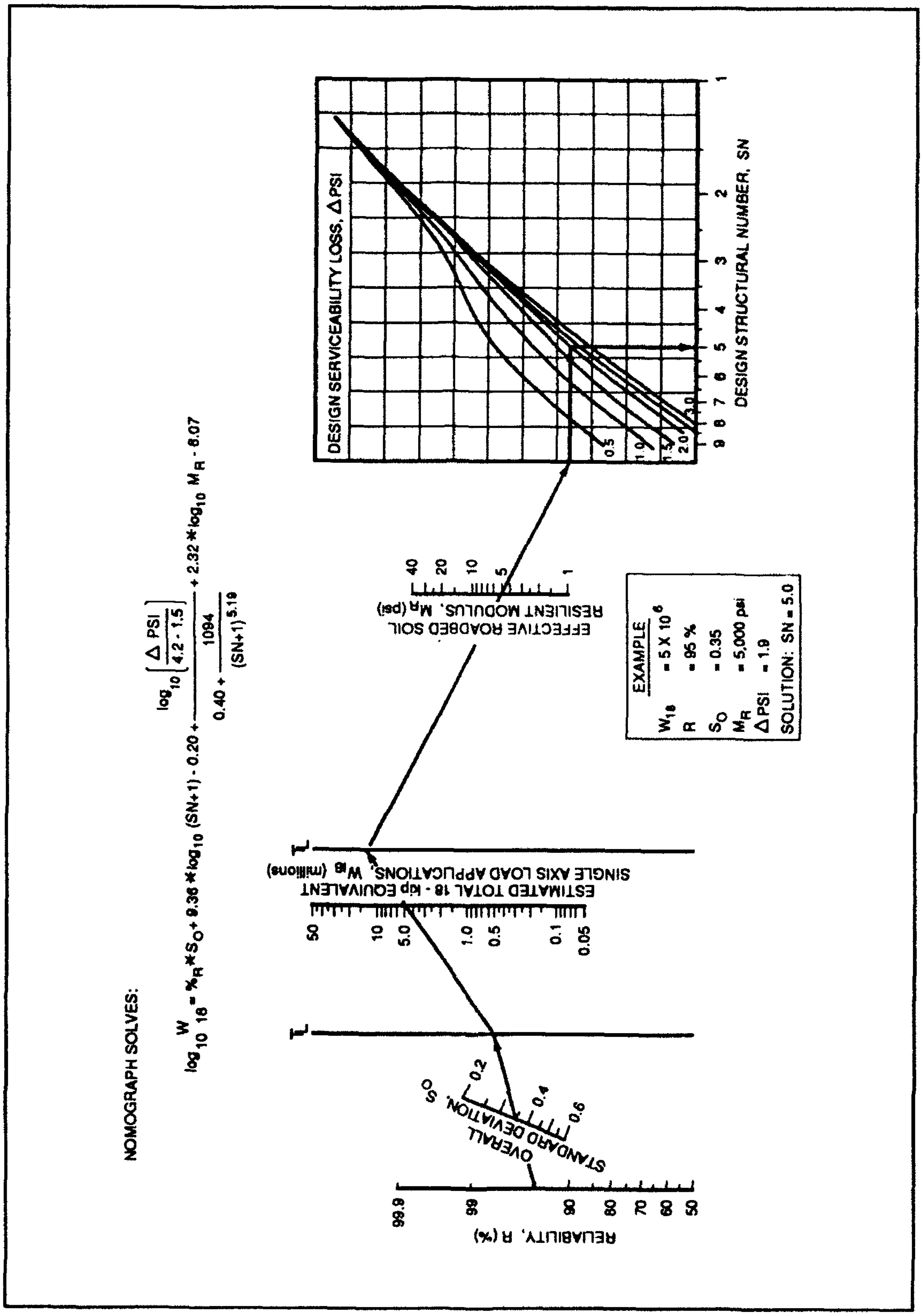

Figure 3. AASHTO design chart for flexible pavements

In an extensive study (ARE, Inc. Engineering Consultants 1989) associated with the development of the FS surface thickness program (STP) the design consultants to the FS evaluated a number of aggregate-surfaced design equations based on the following criteria:

a. Technical validity of the mathematical relationships.

b. Rationality of the input parameters.

c. Utilization of standard traffic units.

d. Availability of material characterization for input.

e. Incorporation of risk/reliability concepts.

f. Type of failure criteria.

g. Incorporation of seasonal change parameters.

h. Incorporation of field experience.

The aggregate-surfaced design methods which were evaluated in the ARE study included methods developed by the Corps of Engineers and the FS. Of all the methods initially reviewed, five were selected for evaluation. These methods are:

a. Corps of Engineers, TM 5-822-12 (Headquarters, Department of the Army 1990).

b. Corps of Engineers (Hammitt 1970).

c. Corps of Engineers (Barber, Odom, and Patrick 1978).

d. FS Surfacing Design and Management System Manual (SDMS) Equations.

e. FS Chapter 50 Design Procedures.

The first two Corps of Engineers design methods are extensions of the original CBR design procedure. The third Corps of engineers design method (Barber, Odom, and Patrick 1978) is a linear regression equation relating an extensive data base of pavement properties to performance. The SDMS equations (USDA FS 1983) are based on a mechanistic-empirical procedure where the layered elastic theory was used to develop equations which were modified using statistical procedures and field performance data. The FS Chapter 50 design procedures are based upon the early forms of the CBR equation (USDA FS 1974). In the evaluation of the applicable design methods the 1978 Corps of Engineers equation was selected, based upon the above criteria, as the best pavement performance model for use in the FS STP design program. The Corps 1978 equation incorporated all the necessary features as

well as providing for upgradability using an enlarged database for recalibration of the regression coefficients. The mathematical formulation for the Corps 1978 equation is given in Chapter 3.

2 Summary of Test Results

General

This chapter summarizes the test results from the traffic applied to the USFS test road. The test road was approximately 0.7 mile in circumference with parallel 12-ft-wide traffic lanes. The test road was divided into 15 test items with a number of curves and grades. The items included one unsurfaced item, five crushed limestone aggregate-surfaced items, and nine AC-paved items. The thicknesses of the items were varied over a wide range. A plan view of the test road is shown in Figure 4. Much of the data collected during the construction and application of traffic was aimed primarily at an observational analysis of the effects of variable tire pressure. With this in mind, it should be noted that not all of the data collected lend to be explicitly used in an analytical investigation of the pavement behavior. A summary of the general characteristics of each item of the test road is shown in Table 1.

Traffic was applied to the test road using two 18-wheeled western style log trucks equipped with a CTI system. The trucks were driven in separate lanes at highway and reduced tire pressure settings, i.e. low- and high-tire pressure. The axle and wheel spacings of these trucks are shown in Figure 5. The outside lane was trafficked with the high pressure tires, and the inside lane was trafficked with the low-pressure tires. The traffic included both loaded and unloaded passes of the trucks with the loaded traffic running in an opposite direction to the unloaded traffic. A summary of the loaded truck weights as used in this analysis is shown in Table 2. No weight measurements were made of the unloaded trucks; therefore, an assumed total weight of 26,000 lb with a steering axle weight of 10,000 lb, and a drive axle weight of 16,000 lb will be used throughout the analysis. For the purposes of analysis, mixed-traffic equivalency relationships will be formulated and applied in Chapter 3.

This chapter presents a general summary of the types of tests conducted as well as representative examples of the data used in the analysis to be presented in Chapter 3. A complete listing of all recorded data and a more detailed description of the test road and vehicle characteristics are presented in Volume I (Grau 1993).

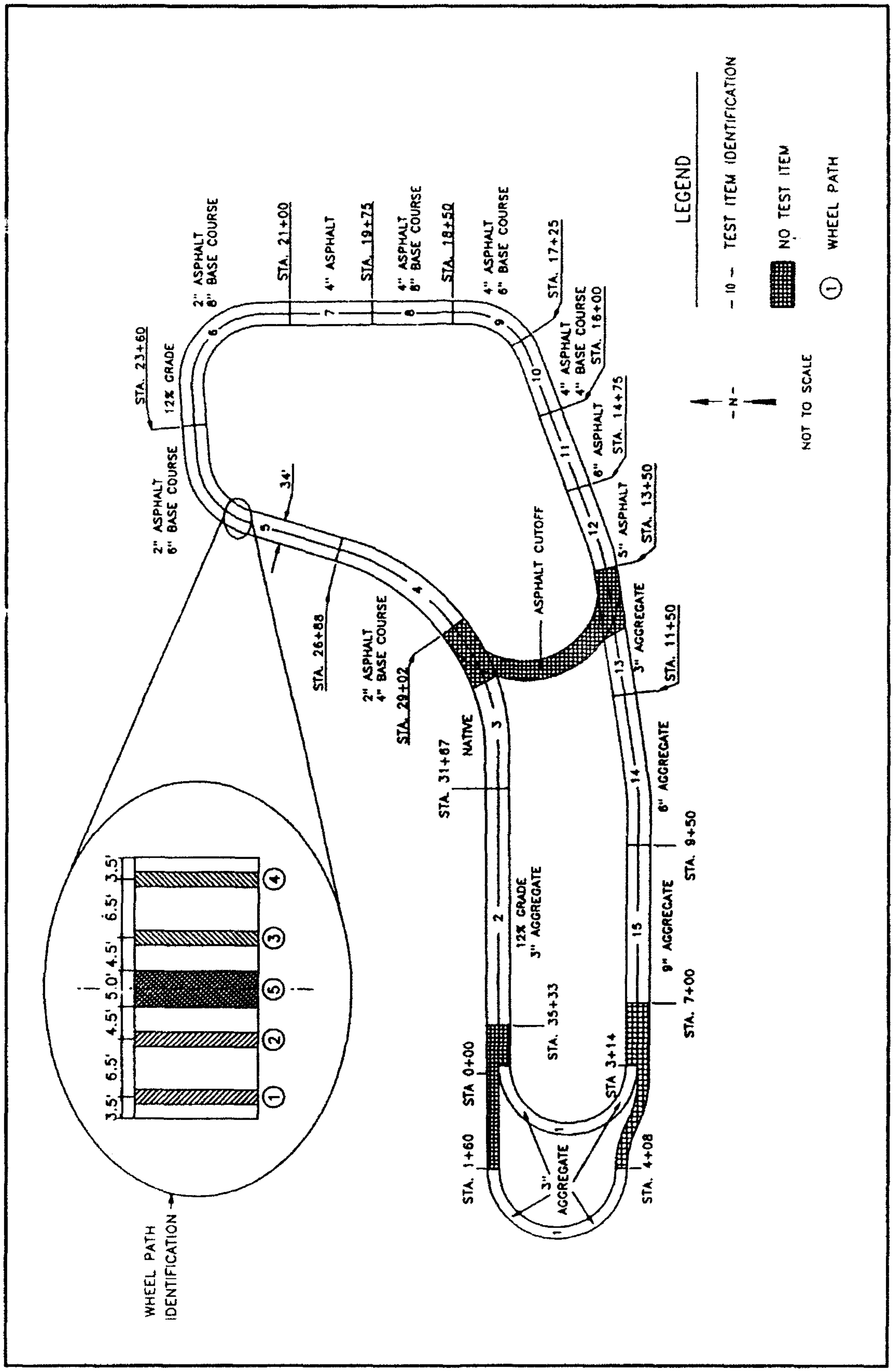

Figure 4. Plan view of test road

Table 1
Properties of Test Items

Item No.	Station		Surface Material	Average Thickness, in.			
				Design		As-Constructed	
	From	To		AC	Aggregate	AC	Aggregate
1	0.00	7.06	Aggregate	NA	3[1]	NA	4.4
2	31.67	35.37	Aggregate	NA	3[1]	NA	3.8
3	29.02	31.67	Unsurfaced	NA	NA[1]	NA	NA
4	26.88	29.02	Asphalt	2	4	2.8	3.0
5	23.60	26.88	Asphalt	2	6	2.7	5.8
6	21.00	23.60	Asphalt	2	8	2.3	5.5
7	19.75	21.00	Asphalt	4	0	5.2	0.0
8	18.50	19.75	Asphalt	4	8	5.0	6.3
9	17.25	18.50	Asphalt	4	6	4.7	5.5
10	16.00	17.25	Asphalt	4	4	4.3	3.6
11	14.75	16.00	Asphalt	6	0	5.7	0.0
12	13.50	14.75	Asphalt	5	0	4.7	0.0
13	11.50	13.50	Aggregate	NA	3	NA	3.0
14	9.50	11.50	Aggregate	NA	6	NA	5.8
15	7.06	9.50	Aggregate	NA	9	NA	7.5

[1] Resurfaced with a 12-in. aggregate overlay after early initial failures.

Native and Aggregate-Surfaced Items

Items 1, 2, 13, 14, and 15 were constructed of compacted crushed limestone. Item 3 was originally constructed of native lean clay material. Items 1, 2, and 3 failed after a small number of passes and were overlaid with 12 in. of aggregate. Only a minimal amount of data was collected on these items after the overlay. Therefore, the majority of data on the aggregate items was taken in items 13, 14, and 15. These items had design thicknesses of 3 in., 6 in., and 9 in. respectively, although the as-constructed thicknesses shown in Table 3 were slightly different from the design values.

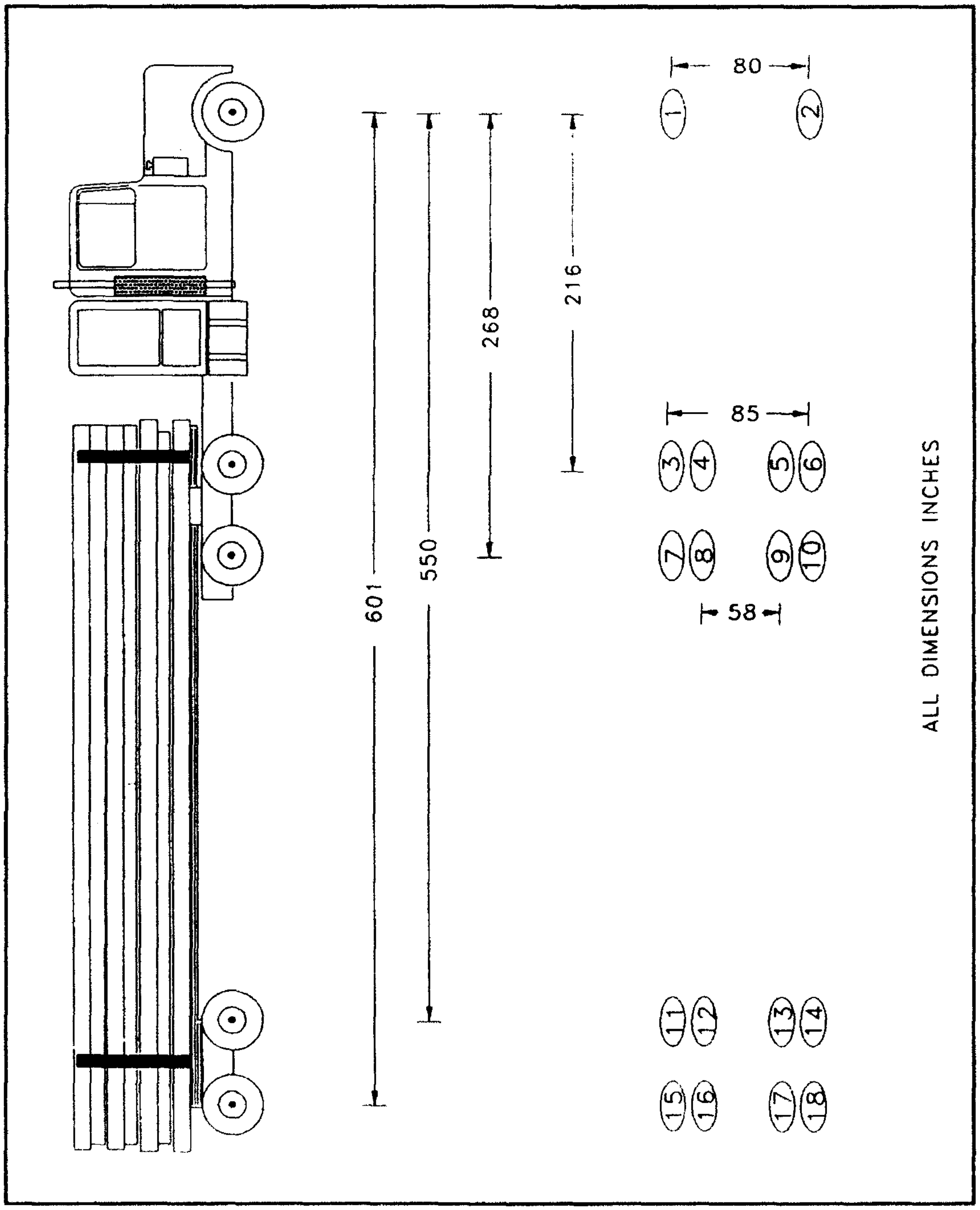

Figure 5. Vehicle dimensions and wheel spacings

Table 2
Loaded Test Truck Characteristics

Axle	Tire Pressure psi	Weight, lb		
		Left	Right	Total
Loaded Test Truck Characteristics				
High Pressure Truck				
Steering	100	4,920	4,670	9,590
Front Drive	100	8,625	8,180	16,805
Rear Drive	10C	8,230	8,200	16,430
Front Trailer	100	7,835	8,520	16,355
Rear Trailer	100	8,415	9,005	17,420
Gross Vehicle Weight	--			76,600
Low Pressure Truck				
Steering	43	4,880	4,650	9,530
Front Drive	39	8,635	8,675	17,310
Rear Drive	39	8,450	8,565	17,015
Front Trailer	38	8,265	8,115	16,380
Rear Trailer	38	8,655	8,500	17,155
Gross Vehicle Weight	--			77,390
Unloaded Test Truck Characteristics				
High Pressure Truck				
Steering	100	5,000	5,000	10,000
Front Drive	100	4,000	4,000	8,000
Rear Drive	100	4,000	4,000	8,000
Gross Vehicle Weight	--			26,000
Low Pressure Truck				
Steering	45	4,880	4,000	10,000
Front Drive	18	4,000	4,000	8,000
Rear Drive	18	4,000	4,000	8,000
Gross Vehicle Weight	--			26,000

Table 3
Properties of Aggregate-Surfaced Test Items

Test Item	As-Constructed Thickness, in.	As Constructed CBR, percent	
		Aggregate	Top of Subgrade
13 High	3.0	35	15
14 High	5.8	32	12
15 High	7.9	32	17

Asphalt-Surfaced Test Items

Items 4, 5, 6, 8 ,9 , 10, and 12 consisted of an AC surface layer with a base course of compacted-crushed limestone on a lean clay subgrade. Items 7 and 11 consisted of an asphalt cement concrete surface layer on a lean clay subgrade. The as-constructed thicknesses of each asphalt-surfaced test item are shown in Table 1.

Rut-Depth Measurements

Periodic rut-depth measurements were made at a minimum of three locations in each wheel path of all test items. Rut-depth measurements were made by measuring the maximum vertical distance from the bottom edge of a straightedge placed on the shoulders (upheaval) of the rut to the bottom of the rut. Figure 6 shows a rut in an aggregate surfaced test item. The rut-depth measurements from a given item and lane at a specific level of traffic were averaged to provide a single rut-depth value for use in the analysis. A more detailed explanation of the test procedures is given in Volume 1.

Cross-Section Measurements

Periodic cross-section elevation measurements were made at the same locations as the rut-depth measurements though not as frequently. These measurements were made using conventional rod and level surveying techniques. A plot of a cross-section profile is shown in Figure 7. These data were used primarily to validate rut-depth measurements by direct comparison and to estimate the amount of traffic channelization by comparing the rut cross section with the wheel spacings.

CBR Strength Measurements

CBR test pits were excavated in each test item in accordance with Army TM 5-530 (Headquarters, Department of the Army 1968). The test pits were located in a nontraffic area along the center line of the roadway at about the midpoint of each test item. These tests were conducted immediately after construction and after a failure occurred in a given test item. The as-constructed CBR data were used directly in the analysis of the aggregate and asphalt test items. A listing of these data is given in Volume 1 of this series of reports.

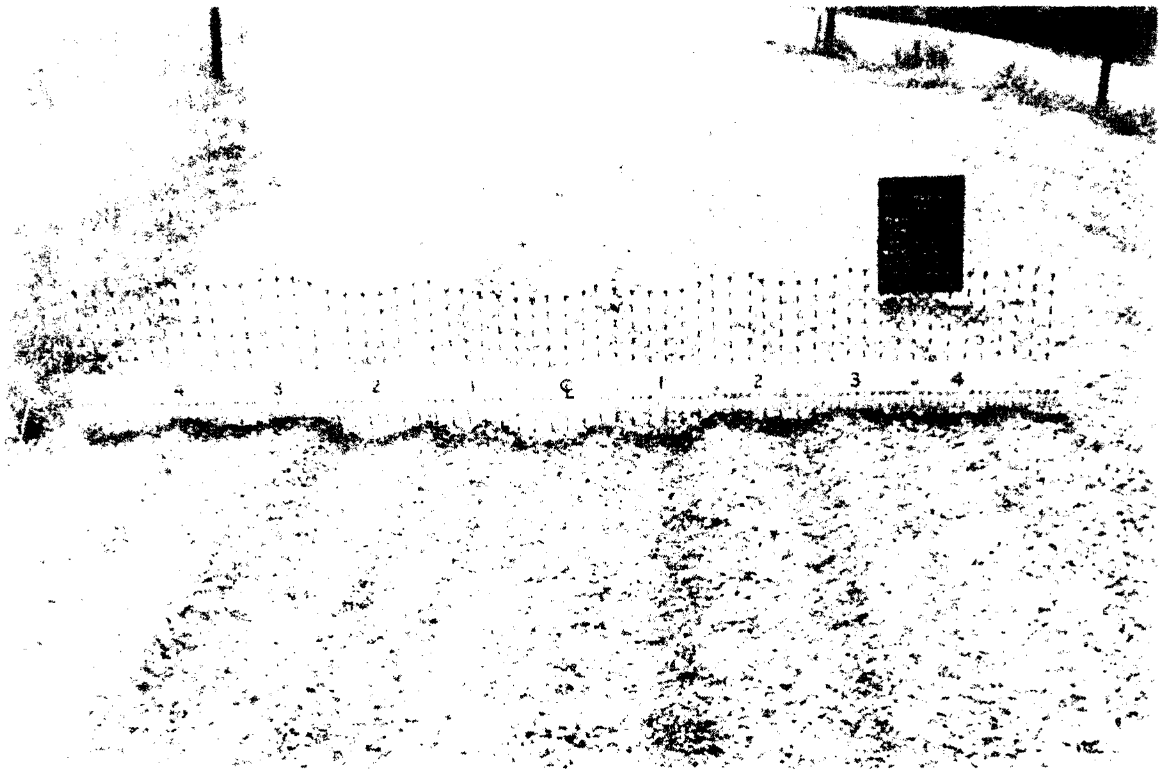

Figure 6. Rutting in an aggregate-surfaced test item

Dynamic Cone Penetrometer Measurements

Dynamic cone penetrometer (DCP) measurements were made at a minimum of three locations in each wheel path (a total of 12) of every test item. In the event of a failure or other inconsistency in behavior under traffic, additional DCP measurements were made. These measurements were made at intervals during the application of traffic in order to maintain some record of the strength of the pavement layers and any strength change associated with traffic, environmental changes, and maintenance of the road surface. These data were converted to equivalent CBR values using Equation 6:

$$CBR = \frac{292}{DCP^{1.12}} \qquad (6)$$

where

CBR = equivalent California Bearing Ratio, percent

DCP = dynamic cone penetration value, mm/blow

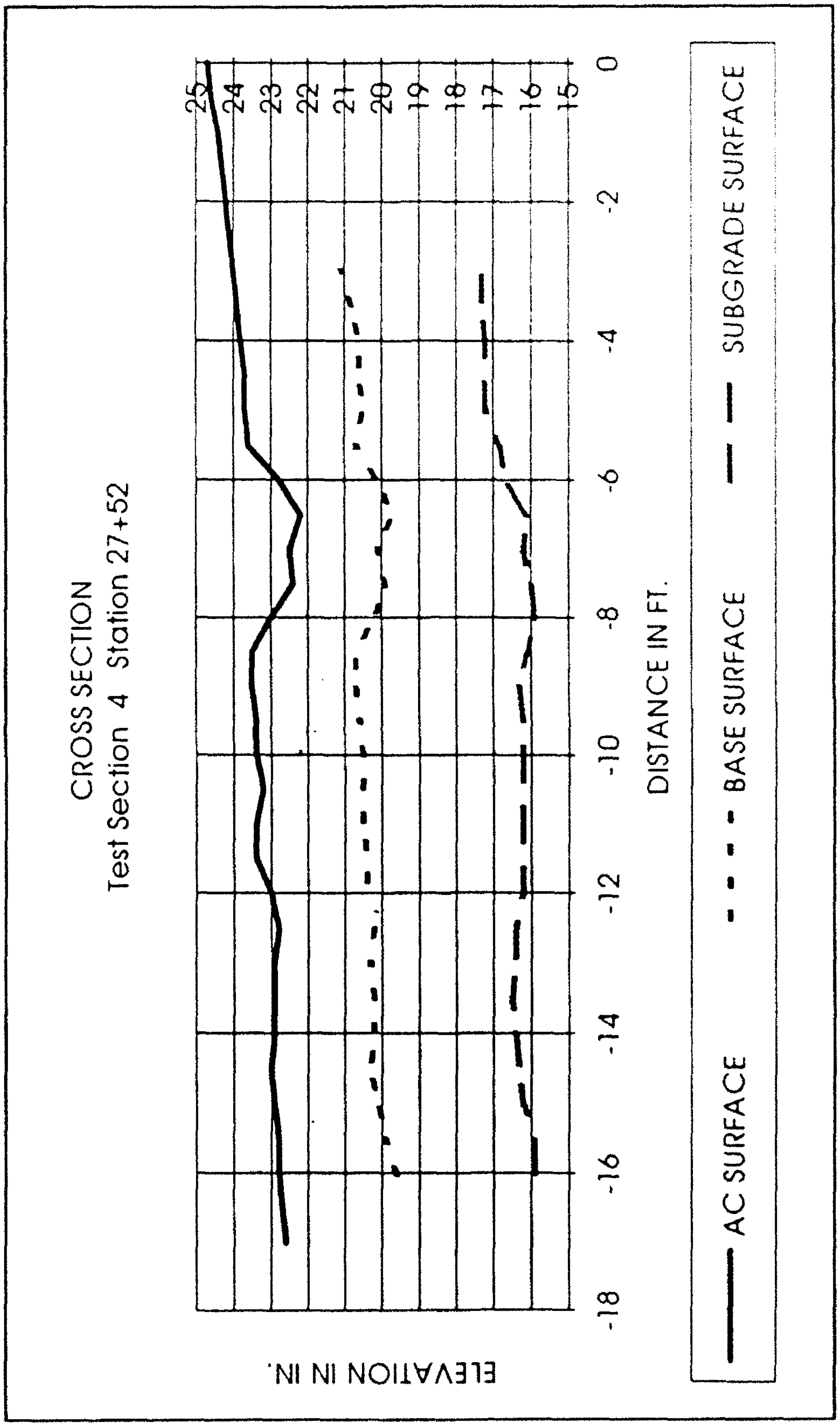

Figure 7. Cross-section plot

The curve from which the CBR versus DCP equation was developed is shown in Figure 8 (Webster, Grau, and Williams 1992). The DCP data were used in the analysis to help assess the cause of any inconsistencies in pavement behavior under traffic, but were not explicitly used to validate any design models since the data are not a direct input parameter in any of the models selected.

Roughness Measurements

The primary method of measuring roughness during the application of traffic was through longitudinal profile surveys of the low- and high-pressure wheel paths of each test item. These data were used in calculating the present serviceability index (PSI) for each item as described in Chapter 3. These data were also used in addressing maintenance issues associated with the effects of tire pressure.

Environmental Data

In order to maintain a record of major changes in pavement condition as a result of temperature and moisture changes, an environmental monitoring station was installed at the test site. This station monitored weather data including temperature, rainfall, relative humidity and wind speed. These data were not used as explicit input parameters in the data analysis but they do provide a great deal of insight into any unusual behavior which might be a result of moisture or temperature fluctuations. A plot of precipitation versus time is shown in Figure 9.

Condition Survey

Periodic pavement condition surveys were conducted for each lane of the test items including both asphalt and aggregate-surfaced sections. These surveys were conducted to determine the change in pavement condition index (PCI) as a function of traffic and tire pressure. These data are not used directly in the analytical effort.

Multidepth Deflectometer Measurements

The multidepth deflectometer is described in detail in Volume 1 of this series. MDD's were installed at locations in items 10 and 12 in the AC-surfaced test items. It allows for real-time deflection measurements to be made in a pavement structure at up to six depths of interest. The MDD's installed at the CTI test road consisted of three measurement modules or sensors. Table 4 gives associated layer thicknesses and MDD locations

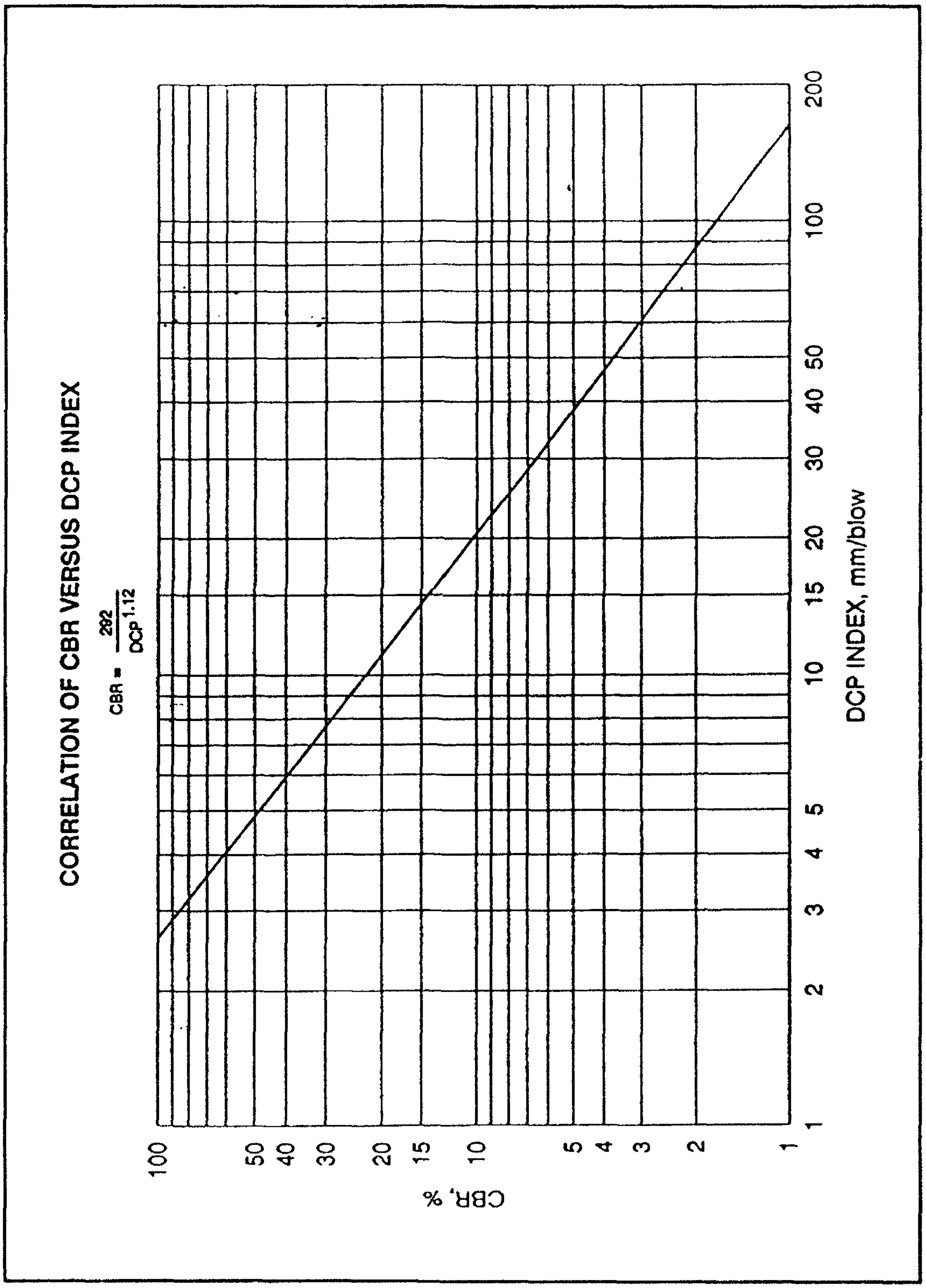

Figure 8. Correlation of CBR versus DCP index

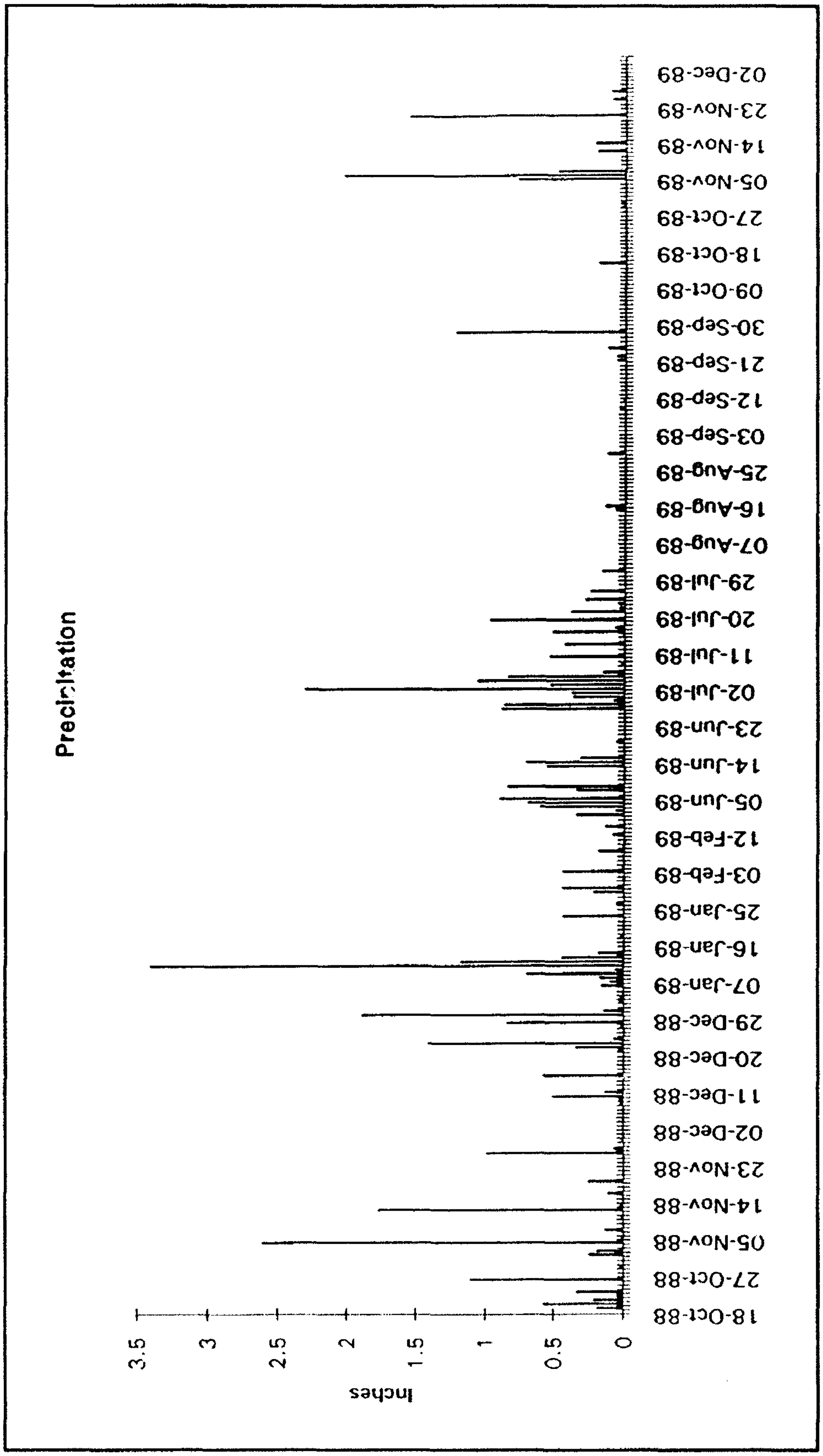

Figure 9. Precipitation in inches versus time

Table 4
Layer Thickness and MDD Locations

Test Item	Layer Thickness[1], in.		Depth of MDD, in.		
	Surface	Base	1	2	3
12	4.7	0.0	5.0	17.25	-
10	4.3	4.0	4.4	10.0	25.9
10	4.3	4.0	4.3	10.4	24.1

[1] Average thickness from high and low lanes.

(Scullion, Bush, and Kenis 1990). Two MDD's were installed in item 10 (one in each lane), and only one MDD was installed in item 12 (high pressure lane). These data were used to assist in calibrating and verifying the mechanistic design model used in the analysis effort. The MDD's provided data on the deflection of the pavement layers at various depths for both elastic and permanent deflections. A sample plot of deflection under a traffic-induced load is shown in Figure 10.

Nondestructive Testing

Falling weight deflectometer (FWD) tests were conducted on all test items at periodic intervals before and during the application of traffic. Layer moduli and associated elastic response parameters were backcalculated from the FWD tests using current layered elastic analysis methods. These properties were used along with CBR, DCP, and laboratory test data to establish the range of elastic properties of the pavement layers for use in the analyses performed.

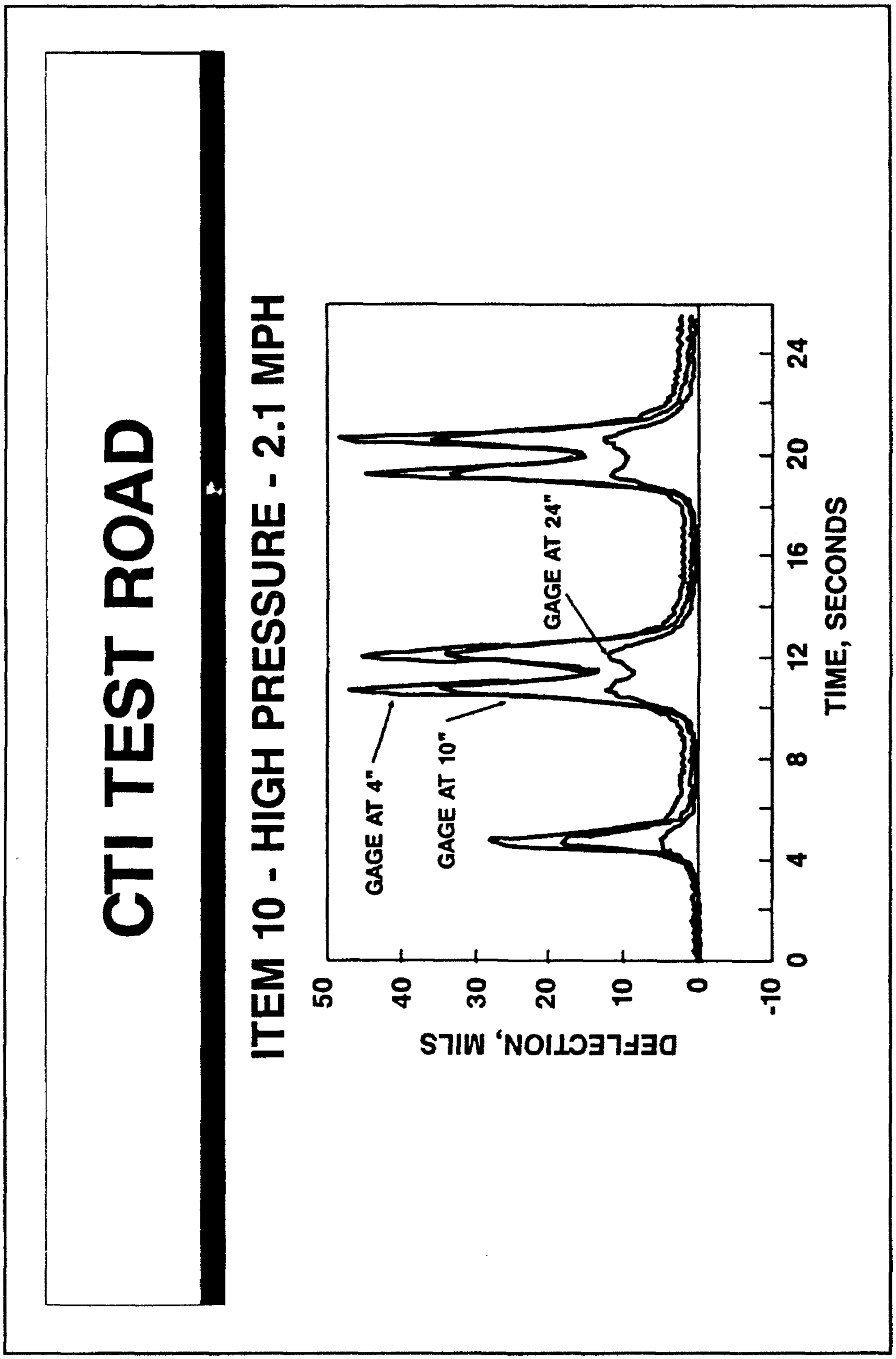

Figure 10. MDD response

3 Analysis of Test Results

General

This chapter describes the analysis of data from both the aggregate and asphalt surfaced test items. The analysis addresses existing design models including both empirical and mechanistic models. The models were calibrated with the necessary data and then compared to the measured results for verification. The design models were used to compute design thicknesses for a number of conditions and their results were compared. A means for addressing the performance of variable tire pressure vehicles on different subgrade and aggregate types were included in the design models and predictions.

Aggregate Surfaced Items

The data from the aggregate-surfaced test items (13, 14, and 15) provide the experimental data necessary for an analysis of the effects of variable tire pressure on aggregate surfaced roads and the applicability of current design procedures under these conditions.

Analysis and selection of design model

As discussed in Chapter 1, the aggregate-surfaced pavement design equation developed by Barber, Odom, and Patrick (1978) is the primary aggregate-surface design equation in use with the FS at this time. Based on a review of alternative methods and recommendations from the FS, the analysis of the test results from the aggregate-surfaced test items were performed using the Corps 1978 model as the major point of emphasis. The equation relates initial pavement material properties to performance using rut depth as the major failure criteria. This equation is shown as Equation 7.

$$(\log t)^{2.002} = (0.1741)\,\frac{P_k^{0.4704}\, t_p^{0.5695}\, R^{0.2476}}{RD\, C_1^{0.9335}\, C_2^{0.2848}} \qquad (7)$$

where

t = aggregate depth, in.

P_k = ESWL, kips

t_p = tire pressure, psi

R = passes of ESWL

RD = rut depth, in.

C_1 = CBR of aggregate surface

C_2 = CBR of subgrade

The data were analyzed such that the results of the test program can be incorporated into the database used to develop the Corps 1978 equation. Once the additional data had been incorporated into the database, the equation coefficients were recalculated using the extended database.

Development of load/pass equivalency concepts

During the application of traffic to the test road both loaded and unloaded trucks were run intermittently creating a condition of mixed traffic. An equivalency relationship between loaded and unloaded traffic for both high pressure and low pressure trucks was developed to handle this aspect of the analysis.

Yoder and Witczak (1975) define an equivalent wheel load factor as the damage per unit pass caused to a specific pavement by the vehicle in question relative to the damage per pass of an arbitrarily selected standard vehicle moving on the same pavement system. This damage can be expressed in terms of deflection, reduction in serviceability, load, or other suitable parameters.

For the purposes of this analysis the concept of an equivalent single-wheel load (ESWL) was used along with the Corps 1978 equation to develop a pass equivalency relationship for the aggregate-surfaced roads. This type of equivalency is needed to convert mixed traffic to a single reference vehicle or wheel configuration. This equivalency relationship is very similar to the existing relationships used in STP 1.02. An equivalent single-wheel load is defined in the Corps design methods as the load on a single tire that will cause an equal magnitude of vertical deflection at a given location within a specific pavement system to that resulting from a multiple-wheel load at the same location within the pavement structure. The contact area of the ESWL was set equal to that of one tire of the multiple gear assembly. The pass equivalency factors are based on the passes of one side of the dual drive wheel tandem axles of a loaded truck as the standard reference load. This is the wheel group of wheels 3, 4, 7, and 8 in Figure 5. This standard loading was

referred to as an equivalent drive axle loading (EDAL). A separate EDAL factor was computed for each truck and lane. The high pressure traffic had a different reference load than the low pressure traffic. This configuration was chosen because of its relationship to the damage (rutting) of the aggregate surface. This standard load is most closely related to the maximum number of stress repetitions that the pavement system experienced due to traffic. The following derivation presents the pass equivalency relationship used for the aggregate-surfaced test items.

Given:

$$(log t) = \left[(0.1741)\,\frac{P_k^{0.4704}\, t_p^{0.5695}\, R^{0.2476}}{RD\, C_1^{0.9335}\, C_2^{0.2848}}\right]^{0.4995} \tag{8}$$

Solving Equation 8 for: **R (passes)**

Equating:

$$R_{reference} = X_f R_{actual} \tag{9}$$

Yields:

$$X_f = \left\{\frac{P_{ku}}{P_{kl}}\right\}^{1.8998} \left\{\frac{t_{pu}}{t_{pl}}\right\}^{2.3001} \tag{10}$$

where

X_f = equivalency conversion factor

P_{ku} = equivalent single-wheel load of wheel group to be converted

P_{kl} = equivalent single-wheel load of reference wheel group

t_{pu} = tire pressure of wheel group to be converted

t_{pl} = tire pressure of reference wheel group

Since this relationship makes use of the Corps 1978 equation, it is only valid in situations where the 1978 equation or its derivatives may be used. For example, the pass equivalency relationship developed should not be used for unsurfaced roads or asphalt-surfaced roads, but is applicable to any aggregate-surfaced roads where the surface CBR is greater than the subgrade CBR. A plot of loaded and unloaded traffic versus time is shown in Figure 11 for the aggregate-surfaced items, and a plot of equivalent traffic (EDAL) versus time is shown in Figures 12 to 14.

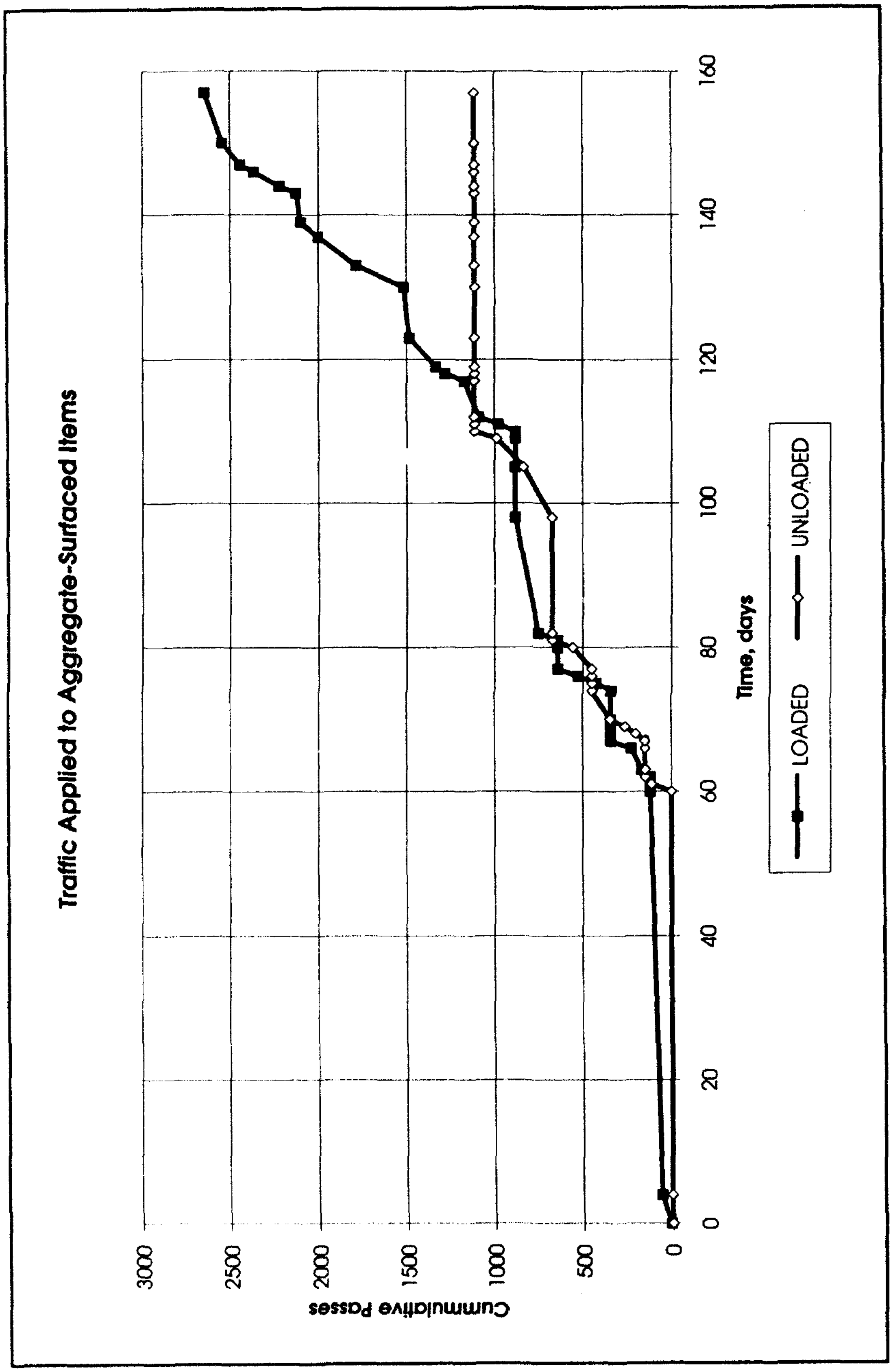

Figure 11. Traffic data from aggregate-surfaced test items

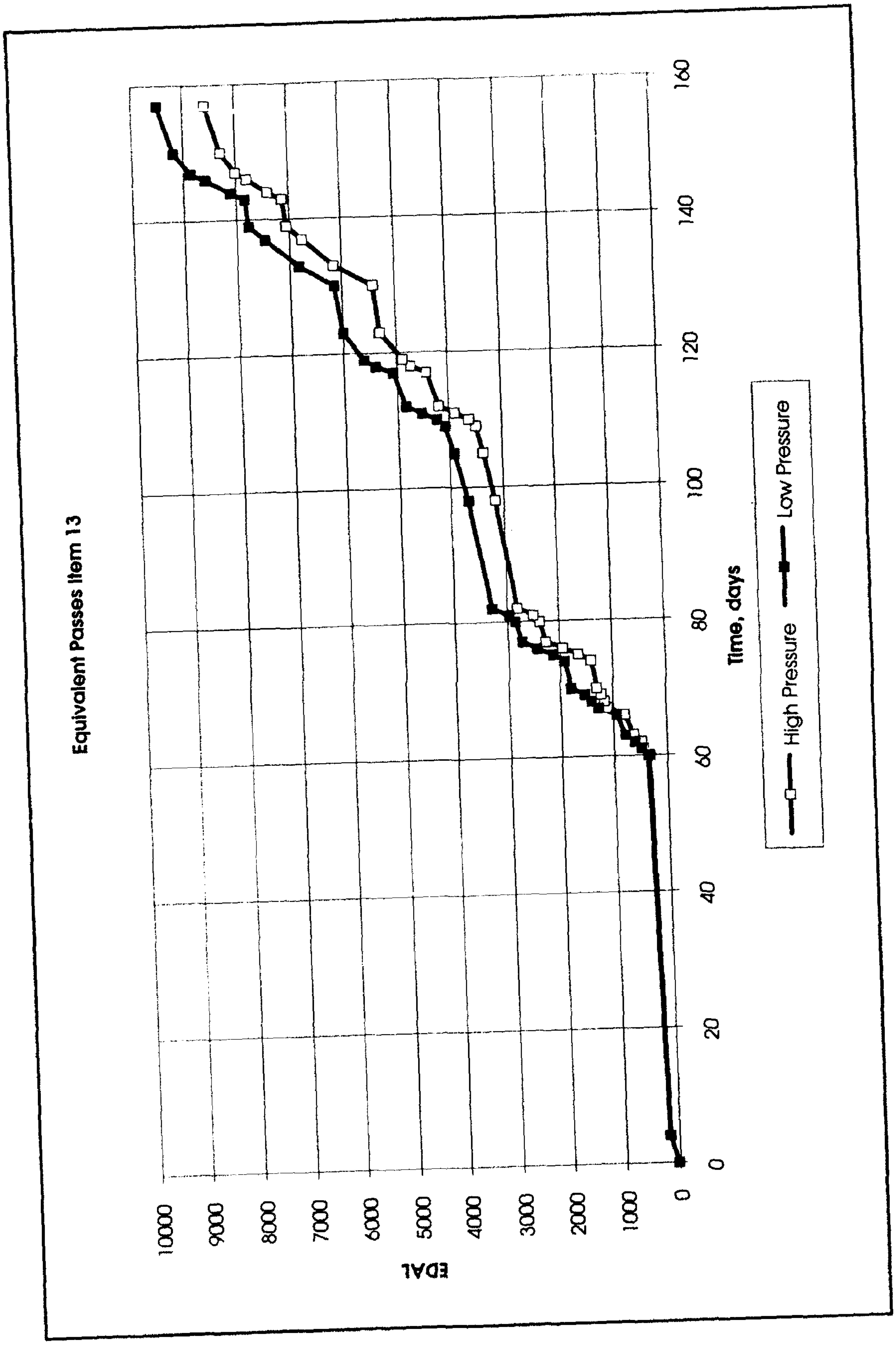

Figure 12. Traffic in EDAL for Item 13

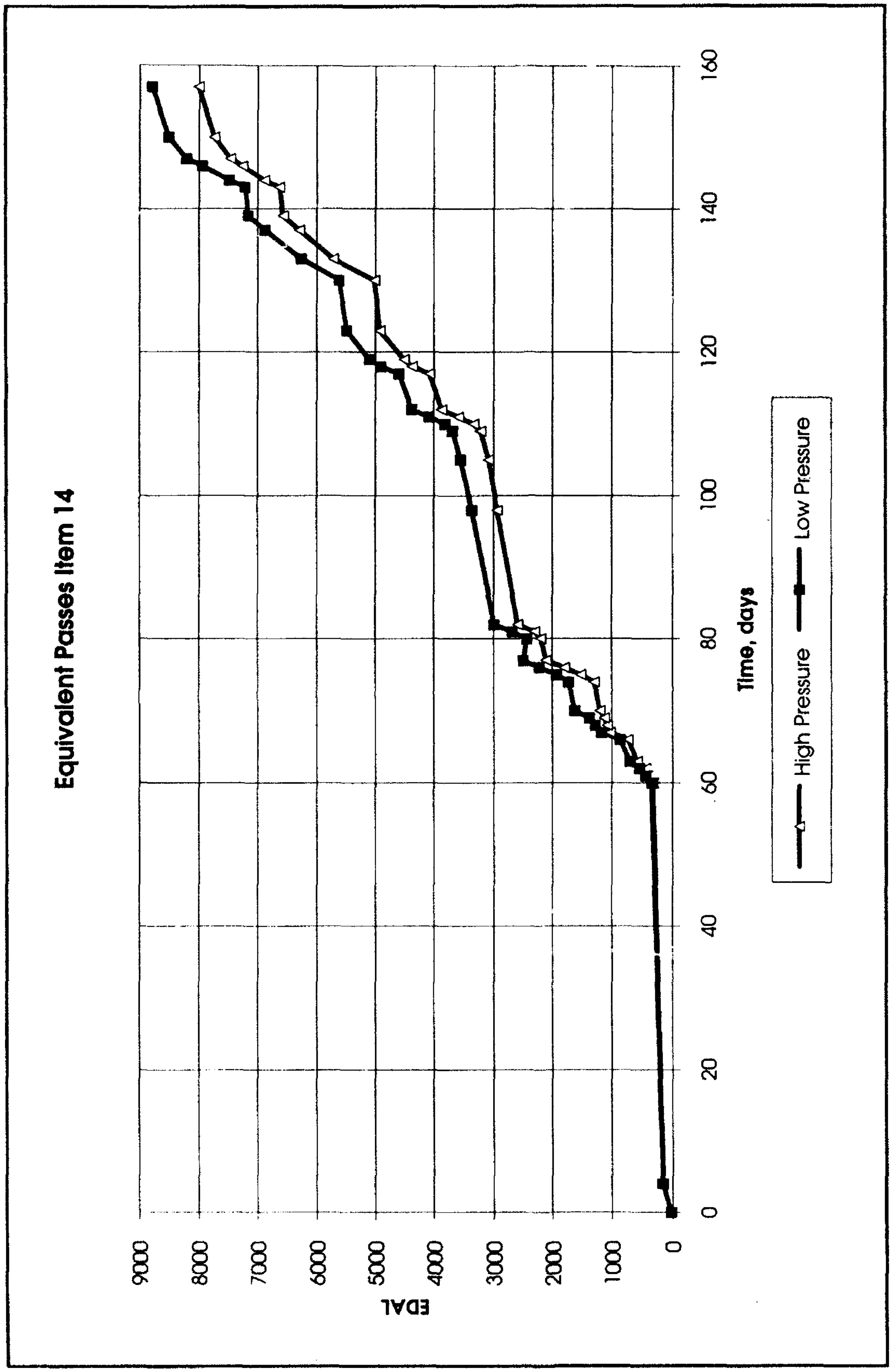

Figure 13. Traffic in EDAL for Item 14

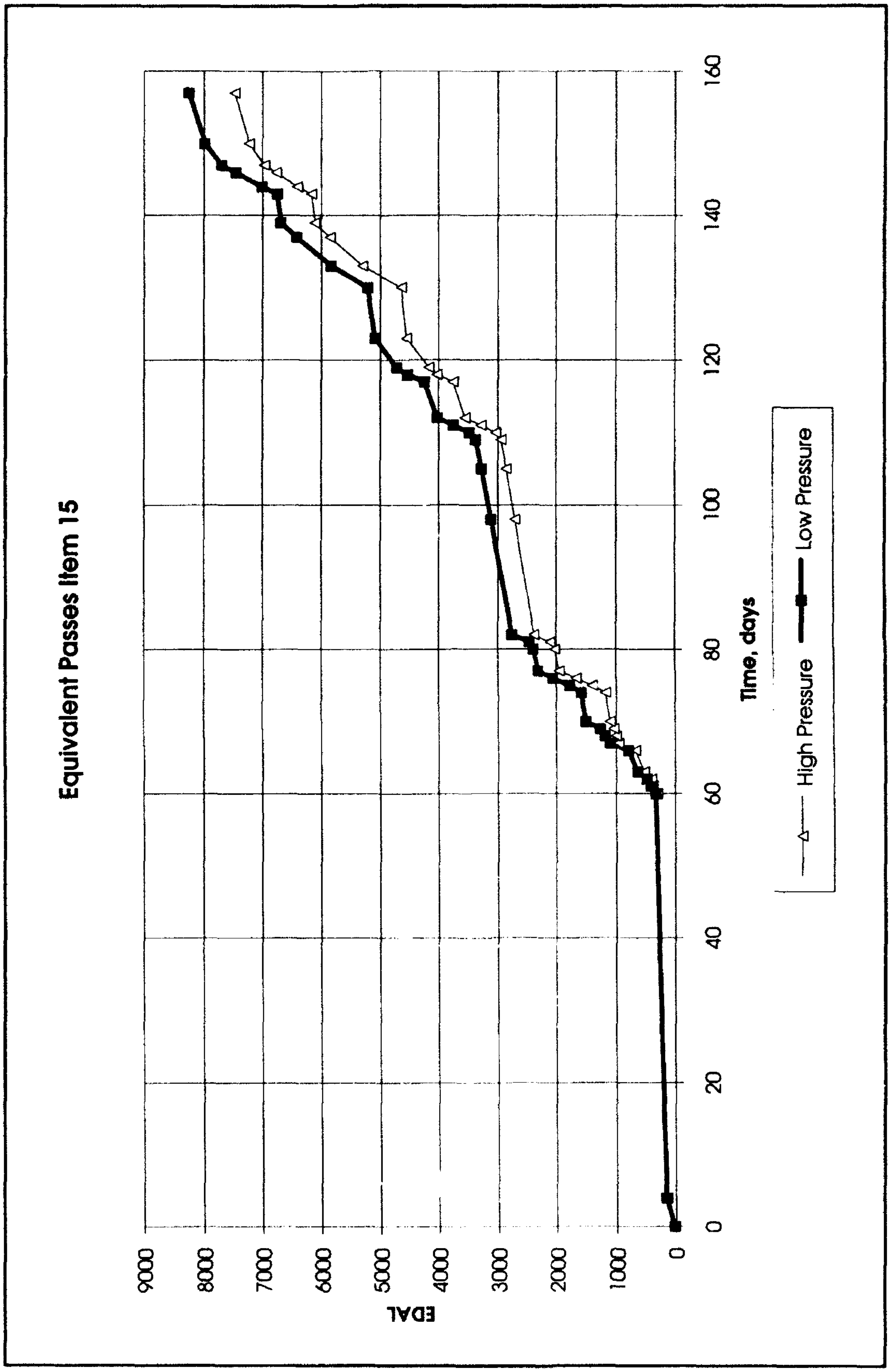

Figure 14. Traffic in EDAL for Item 15

Calibration and verification of design model

The basic failure parameter in the Corps 1978 equation is rut depth. When failures occurred during the application of traffic, the road surface was graded to a smooth condition. Although DCP measurements were made after each grading, no CBR test pits were excavated, nor were any thickness measurements performed in the test items. Since these are the major pavement failure parameters found in the Corps 1978 equation, it was decided to use only that data taken before grading to update the model. Some general observations of data trends after grading of the road surface were noted. In Figures 15 to 17 a general trend towards a more random distribution of rut depth can be seen, although the rate of rut increase is somewhat larger than that seen in the prefailure portion of the data for all three test items. The average rut depth at a given pass level becomes larger where the as-constructed aggregate layer thickness is smaller (for example, the average rut depth at 8000 EDAL is largest in item 13 and smallest in item 15).

The original Corps 1978 model relates a number of pretraffic conditions to overall pavement performance with rut depth as the major failure parameter. Because of this, the as-constructed CBR values at the top of a given layer were used for the analysis, although it is common practice to use a rated CBR based on an average of CBR within a given material over the duration of traffic. This practice of using a surface pretraffic CBR value is in line with the FS-aggregate surface design methods being investigated. A total of 19 data points were added to the existing 254 point database used in the original development of the Corps 1978 equation. The complete database is presented in Appendix A, and the additional points from the FS-CTI test road are given in Table 5.

The Corps 1978 equation was developed using a multiple linear regression technique as described in Barber, Odom, and Patrick (1978). A similar technique was used to perform a multiple linear regression of seven variables for the combination of the original database and the FS-CTI data. During the development of the original design equation rut depth was treated as the dependent variable about which the regression was performed. The equation for rut depth was then algebraically transformed into an equation for thickness. The algebraic manipulation of a multiple linear regression equation is mathematically possible but may not yield the most statistically correct equation. Following the method presented by Hammitt et al. (1971) the new data were added to the original database, and a multiple linear regression was performed twice. The first regression was performed to find an equation for rut depth in terms of the other six variables. The result is Equation 11 which will be referred to as R92:

$$RD = (0.1090) \frac{P_k^{0.4988} \, t_p^{0.5641} \, R^{0.2418}}{(log t)^{1.567} \, C_1^{0.9169} \, C_2^{0.0365}} \tag{11}$$

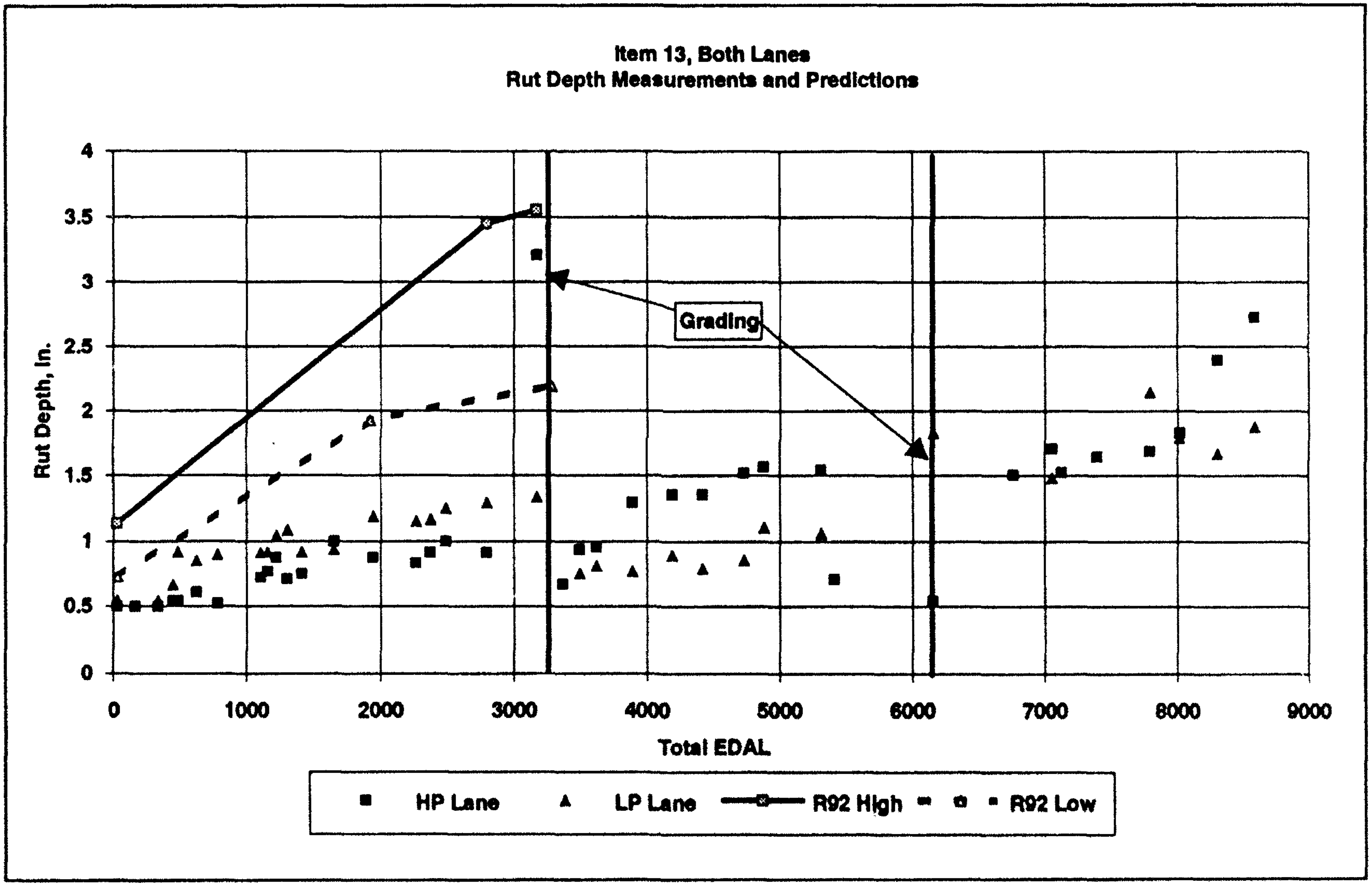

Figure 15. Measured and predicted rut depth versus traffic for Item 13

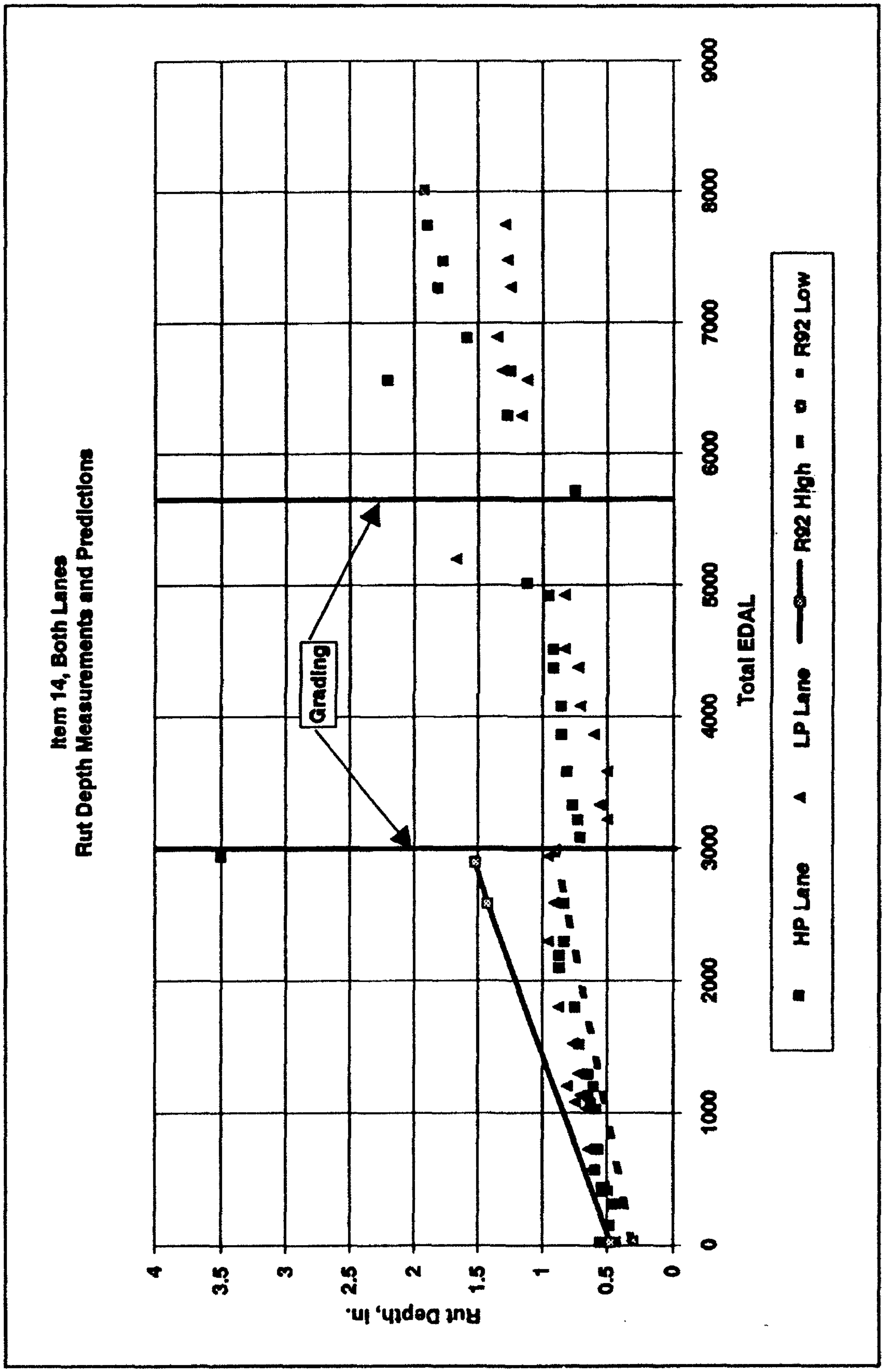

Figure 16. Measured and predicted rut depth versus traffic for Item 14

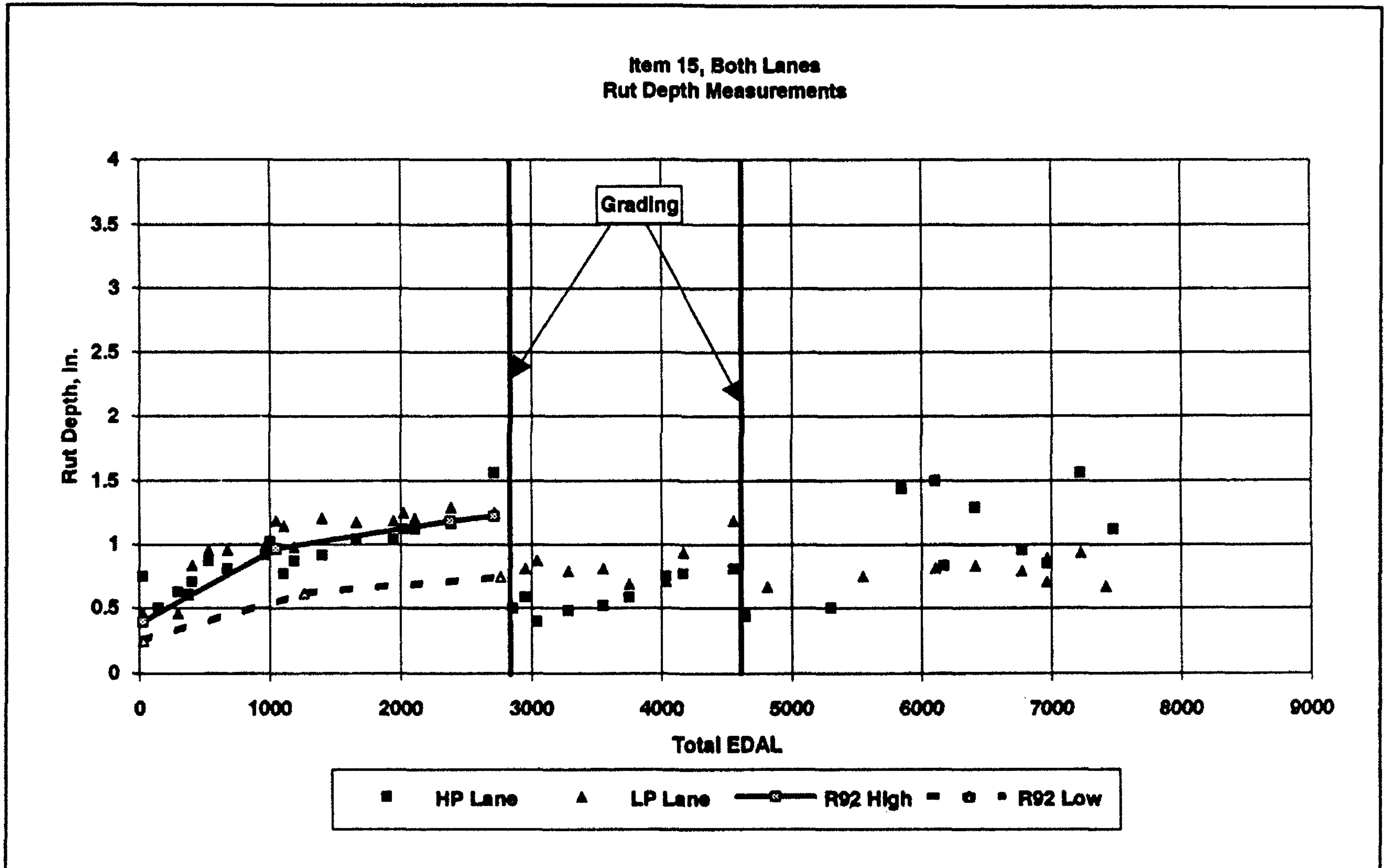

Figure 17. Measured and predicted rut depth versus traffic for Item 15

Table 5
Aggregate-Surfaced Test Results

Data Point	Rut Depth, in.	ESWL kips	Tire Pressure, psi	Aggregate Thickness, in.	As-Constructed CBR, percent		Repetitions
					Aggregate	Subgrade	
1	0.50	5.530	100	2.50	35	15	28
2	0.92	5.530	100	2.50	35	15	2,800
3	3.21	5.5030	100	2.50	35	15	3,172
4	0.504	5.990	39	2.50	35	15	34
5	0.94	5.990	39	2.50	35	15	1,920
6	1.33	5.990	39	2.50	35	15	3,286
7	4.21	5.990	39	2.50	35	15	3,672
8	0.77	6.215	100	5.75	32	12	27
9	1.38	6.215	100	5.75	32	12	2,589
10	0.67	6.762	39	5.75	32	12	32
11	1.500	6.762	39	5.75	32	12	2,991
12	0.88	7.129	100	7.50	32	17	25
13	1.77	7.129	100	7.50	32	17	1,046
14	2.04	7.129	100	7.50	32	17	2,385
15	3.17	7.129	100	7.50	32	17	2,717
16	0.83	7.603	39	7.50	32	17	31
17	2.11	7.603	39	7.50	32	17	1,266
18	2.38	7.603	39	7.50	32	17	2,764
19	3.04	7.603	39	7.50	32	17	3,115

The second regression was performed to find a statistically accurate equation relating the log of thickness to the other six variables with the result being given in Equation 12 which will be referred to as T92:

$$\log(t) = (0.2959)\ \frac{P_k^{0.2016}\ t_p^{0.2481}\ R^{0.0747}}{RD^{0.2128}\ C_1^{0.2414}\ C_2^{0.0596}} \tag{12}$$

The two new equations will be referred to as R92 for the rut depth equation and T92 for the thickness equation. A plot of predicted rut depth (R92) and measured rut depth versus EDAL is shown in Figures 15 to 17 for both lanes of items 13, 14, and 15. The terms "High Pred., Low Pred., etc.," refer to the rut depth values predicted using equation R92. A plot of predicted (R92) versus measured rut depth is shown in Figure 18. These data are presented for measurements prior to failure and subsequent maintenance of the road surface. A comparison of the Corps 1978 equation and T92 is shown in Figure 19. The pronounced effect of tire pressure on design thickness is shown in Figure 20. Equation C78 shows a lower required thickness than equation T92. This difference is significant and can be most significantly attributed to the fundamental difference in the way the equations were obtained, where T92 is a direct result of a multiple linear regression and the C78 thickness equation is a result of an algebraic manipulation of a multiple

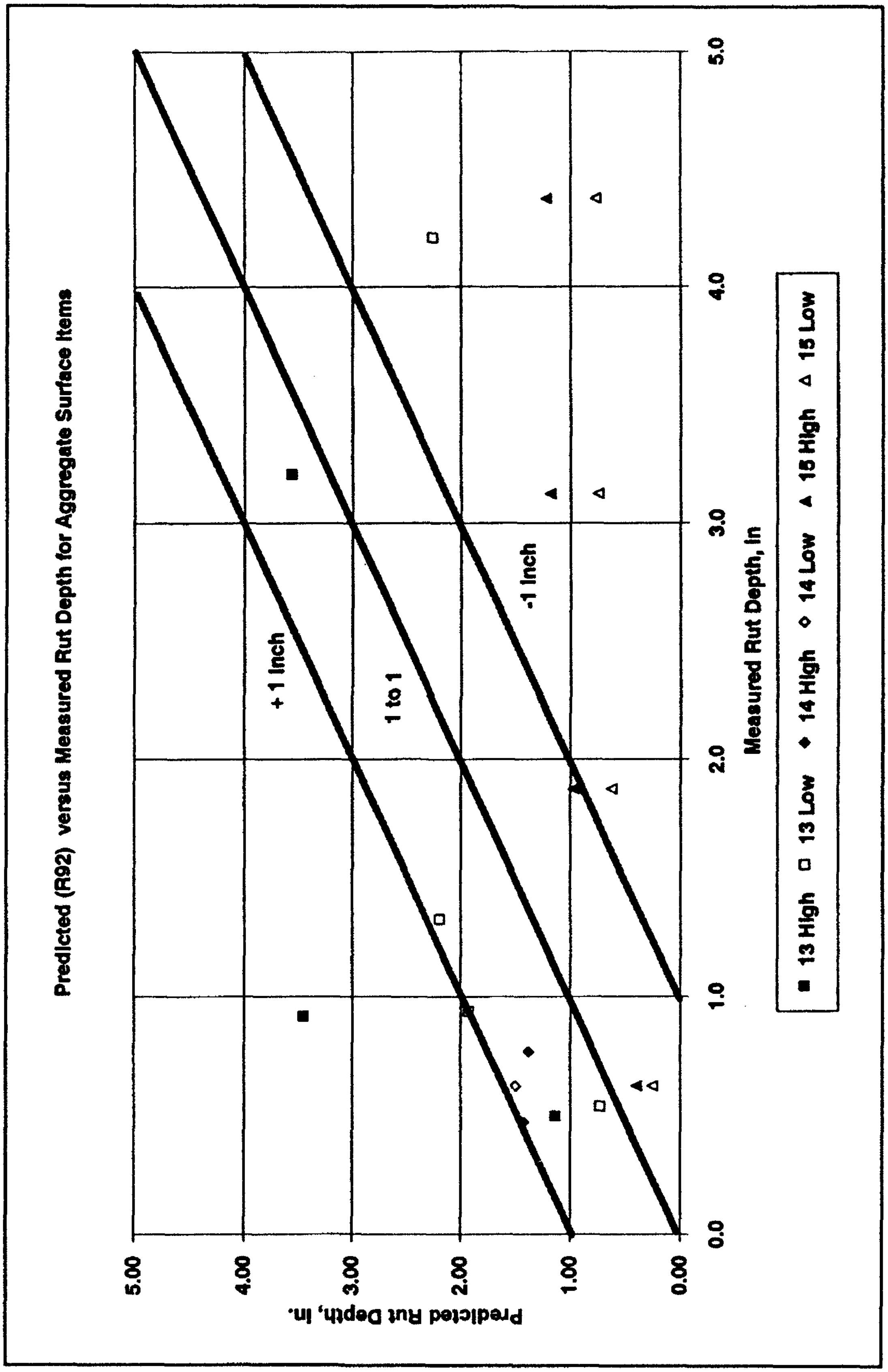

Figure 18. Predicted (R92) versus measured rut depth for aggregate-surfaced test items

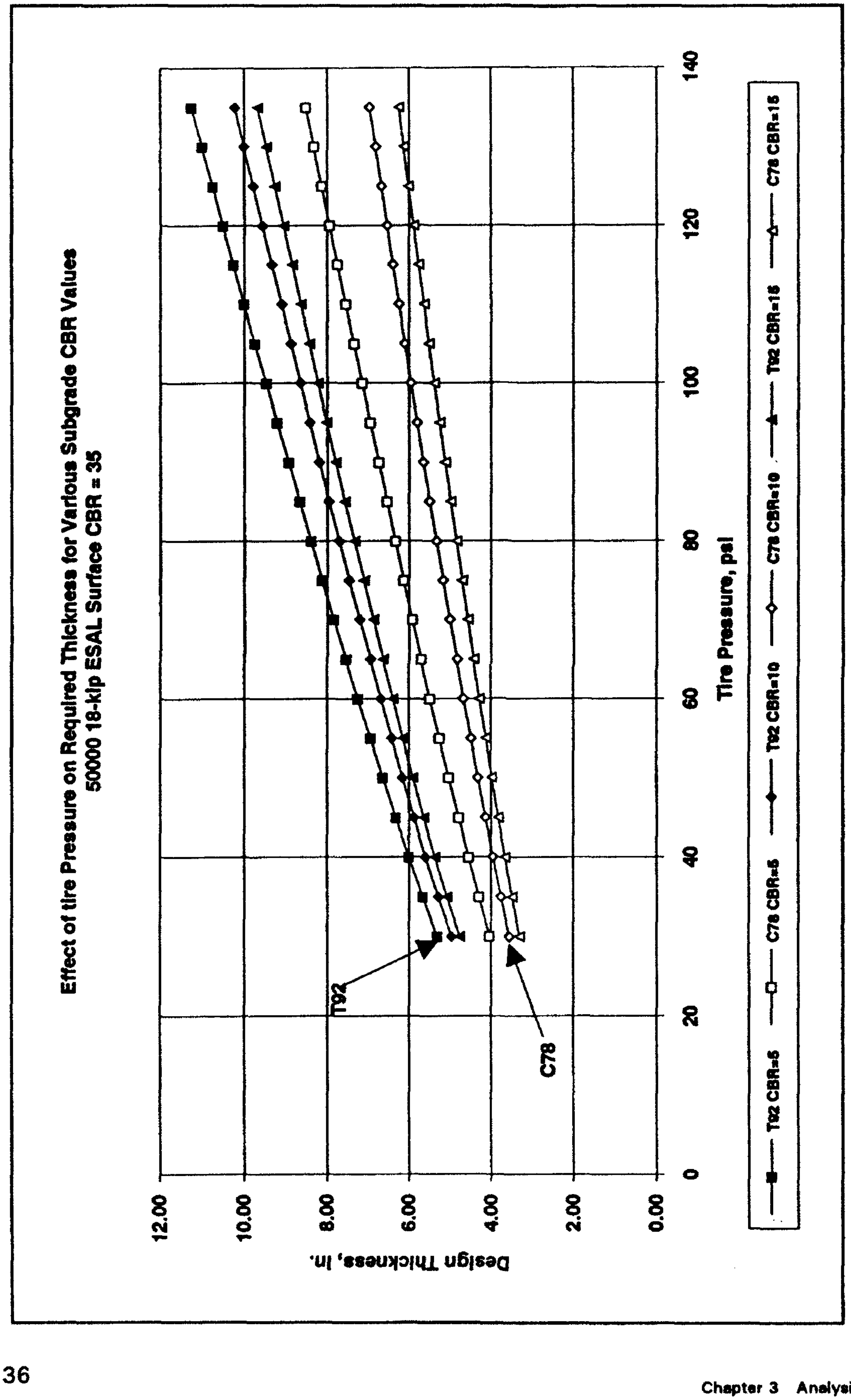

Figure 19. Comparison plot of C78 and T92 equations

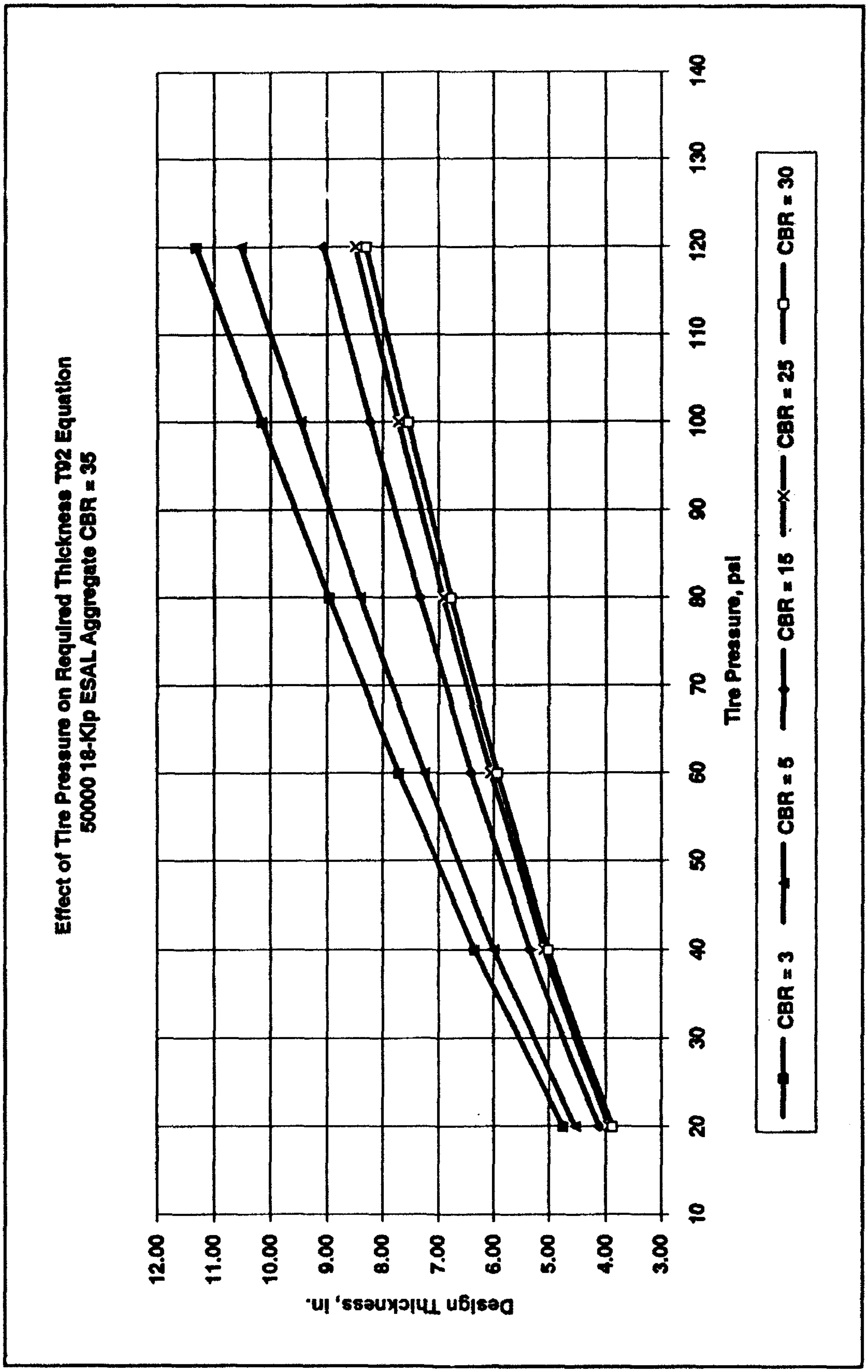

Figure 20. Plot of T92 equation showing the effect of tire pressure on design thickness

linear regression. A multiple linear regression utilizes the concept of residual minimization about a single dependent variable. This type of procedure produces a mathematically coupled equation in which the variables are not completely independent and therefore cannot be algebraically manipulated to form other statistically accurate relationships. Although such an algebraically derived equation would be mathematically correct, it is not as statistically accurate as a relationship obtained from direct multiple linear regression.

Asphalt Concrete Surfaced Items

The data from the AC surfaced sections of the CTI test road provide the basis for an analysis of the effects of variable tire pressures on low volume AC surfaced roads. Both empirical and mechanistic models were used in the data analysis. The structural and material property parameters in these models were calibrated with laboratory or filed measurements and compared with actual field performance data. Detailed descriptions of the trends in pavement behavior under traffic are given in Volume 1 of this series.

Empirical models

A number of flexible pavement design models were noted in the review of previous work. Of the empirical models investigated, the Corps of Engineers flexible pavement design equation and the AASHTO flexible pavement design equation were used in the analysis of the AC test items. Many of the parameters necessary for calibration of the empirical design models appear to be the same property with different values. These differences are a result of a different set of conversion and equivalency relationships used with a given design method.

AASHTO flexible pavement design equation

The AASHTO flexible pavement design equation was chosen since it is the most widely used flexible pavement model in the FS. The AASHTO flexible pavement design equation is given in Equations 4 and 5:

$$Log_{10}W_{18} = R(S_o) + 9.36\ Log_{10}(SN + 1) - 0.20 + \left[\frac{Log_{10}\left[\dfrac{\Delta PSI}{4.2 - 1.5}\right]}{0.4 + \left[\dfrac{1094}{(SN + 1)^{5.19}}\right]}\right] + 2.32\ Log_{10}M_R - 8.07 \qquad (4\ \text{bis})$$

$$SN = a_1D_1 + a_2D_2 + a_3D_3 \qquad \text{(5 bis)}$$

where

W_{18} = traffic in 18-kip equivalent single-axle loads

R = reliability factor in percent

S_o = standard deviation of traffic and performance prediction

S_N = structural number

ΔPSI = change in present serviceability index

M_R = resilient modulus of the subgrade in psi

a_i = i^{th} layer coefficient

D^i = i^{th} layer thickness, in.

The structural number is an abstract number expressing the strength of a pavement required for a given combination of soil strength, traffic, terminal serviceability, and environment.

AASHTO equivalency factors

As was the case with the aggregate-surfaced test items, traffic was also applied to the AC test items with both loaded and unloaded vehicles. The AASHTO design guide provides a detailed method for converting mixed vehicle traffic to standard 18-kip ESAL. The procedure uses vehicle loads, axle types, pavement structural number, and terminal serviceability index to compute ESAL's from a mixed traffic count. Structural layer coefficients were determined using field and laboratory data in conjunction with the charts given in Figures 21 and 22 (AASHTO 1986). These coefficients along with the layer thicknesses of the AC test items were used to compute structural numbers for each test item. For a terminal serviceability index of 2.5 the charts shown in Figures 23 and 24 were used to compute the 18-kip ESAL equivalency factors given in Table 6, which were then applied to the actual traffic data to compute traffic in ESAL's. This method of computing equivalent traffic is simple and effective; however, it should only be used in conjunction with the AASHTO analysis/design procedures. The following is an example of the determination of one of the 18-kip equivalency factors given in Table 6.

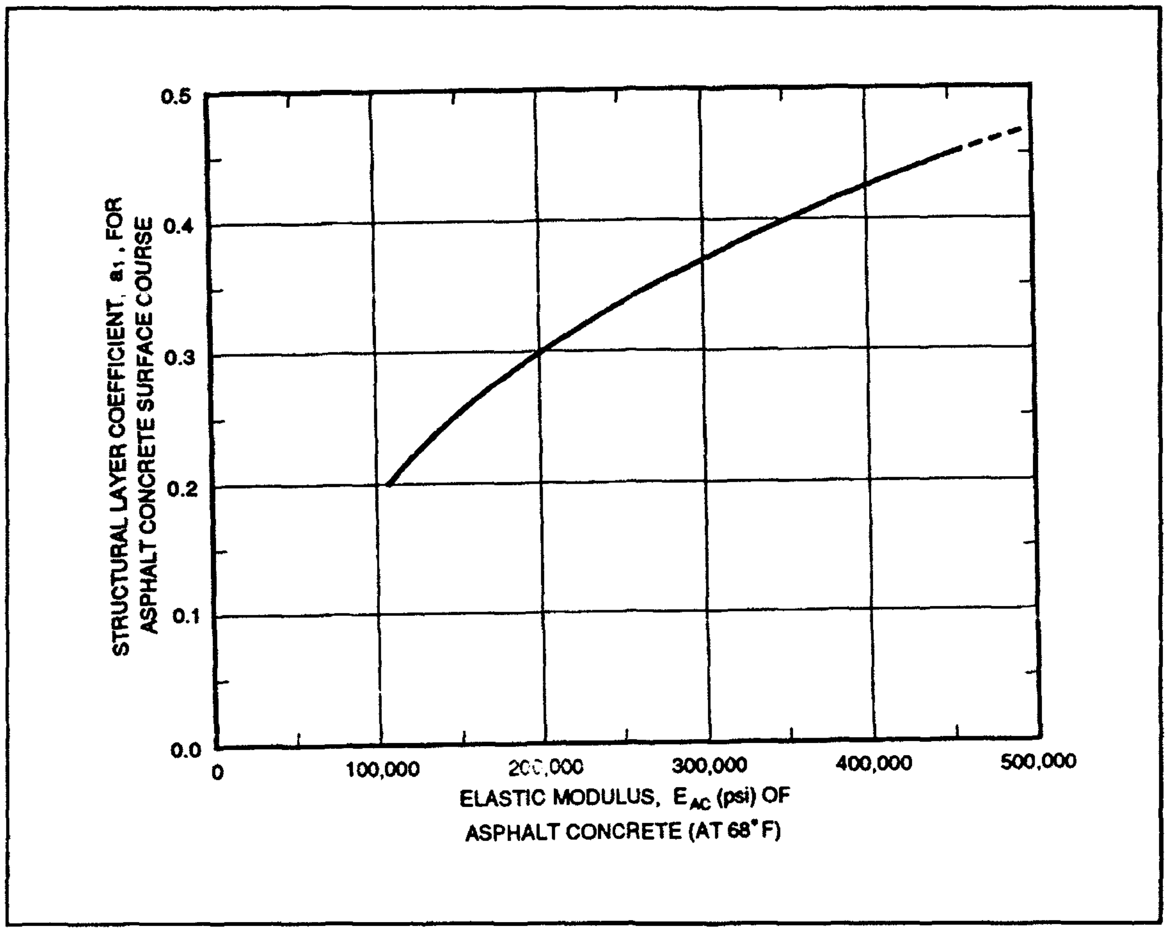

Figure 21. Chart for estimating structural layer coefficient of dense-graded AC based on elastic (resilient) modulus (AASHTO 1986)

Given the following information:

Item:	5 (SN = 1.22)
Vehicle:	Loaded high pressure
	1 single axle at 9,500 lb
	2 tandem axles at 34,000 lb each

Yields equivalency factors from Figures 23 and 24:

Single axle	= 0.069
Dual axle	= 1.06 (2 each)
Total factor	= 2.19

Calibration and verification of AASHTO design procedures

The AASHTO failure criterion is based on an allowable reduction in PSI for a given pavement. PSI is defined as a function of pavement rut depth, roughness, cracking, and patching. Due to the nature of the equation for PSI, the roughness is the parameter that causes the greatest change in PSI, although

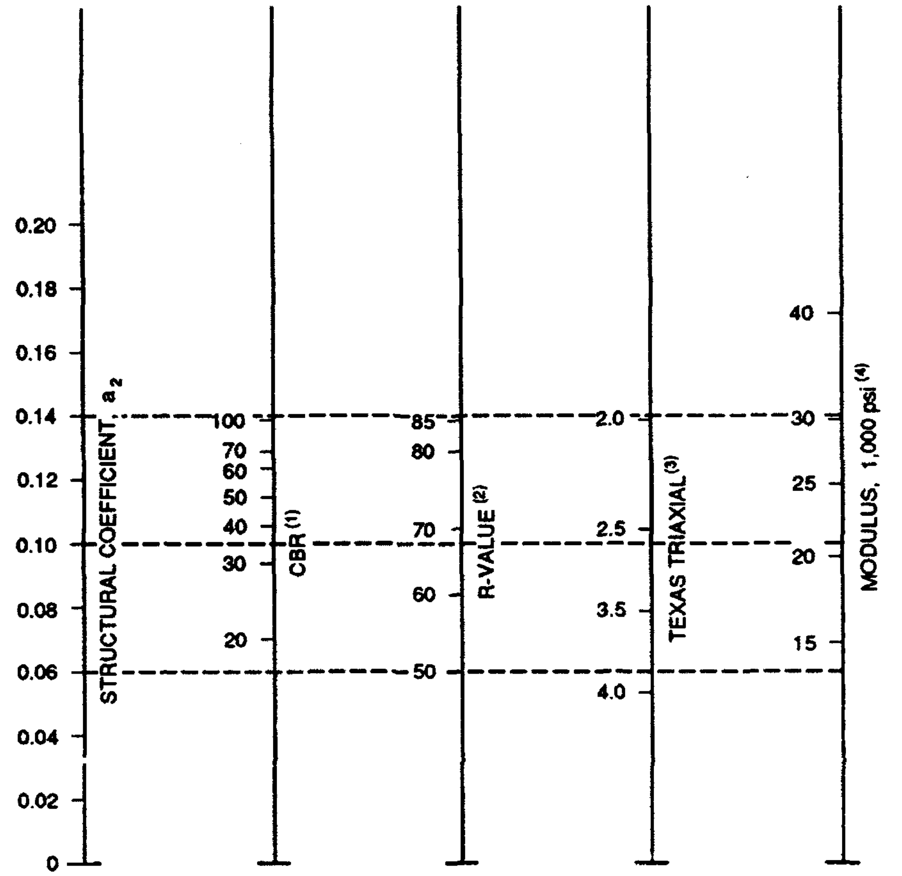

Figure 22. Variation in granular base layer coefficient (a_2) with various base strength parameters (AASHTO 1986)

the cracking, patching, and rutting parameters were still used in the calculation. It is normally assumed to follow a pattern as shown in Figure 25. Pavement roughness is defined by variations in the longitudinal profile of the pavement surface as shown in Equation 13a and b:

$$PSI = 5.03 - 1.9 Log(1 + SV) - 0.01\sqrt{C + P} - 1.38\overline{RD}^{2} \qquad (13a)$$

Axle Load (kips)	Pavement Structural Number (SN)					
	1	2	3	4	5	6
2	.0004	.0004	.0003	.0002	.0002	.0002
4	.003	.004	.004	.003	.002	.002
6	.011	.017	.017	.013	.010	.009
8	.032	.047	.051	.041	.034	.031
10	.078	.102	.118	.102	.088	.080
12	.168	.198	.229	.213	.189	.176
14	.328	.358	.399	.388	.360	.342
16	.591	.613	.646	.645	.623	.606
18	1.00	1.00	1.00	1.00	1.00	1.00
20	1.61	1.57	1.49	1.47	1.51	1.55
22	2.48	2.38	2.17	2.09	2.18	2.30
24	3.69	3.49	3.09	2.89	3.03	3.27
26	5.33	4.99	4.31	3.91	4.09	4.48
28	7.49	6.98	6.90	6.21	6.39	6.98
30	10.3	9.5	7.9	6.8	7.0	7.8
32	13.9	12.8	10.5	8.8	8.9	10.0
34	18.4	16.9	13.7	11.3	11.2	12.5
36	24.0	22.0	17.7	14.4	13.9	15.5
38	30.9	28.3	22.6	18.1	17.2	19.0
40	39.3	36.9	28.5	22.5	21.1	23.0
42	49.3	45.0	35.6	27.8	25.6	27.7
44	61.3	55.9	44.0	34.0	31.0	33.1
46	75.5	68.8	64.0	41.4	37.2	39.3
48	92.2	83.9	65.7	50.1	44.5	46.6
50	112.	102.	79.	60.	53.	55.

Figure 23. AASHTO table of load equivalency factors for flexible pavements, single axles, and terminal serviceability index of 2.5 (AASHTO 1986)

$$SV = \frac{\Sigma Y^2 - \left[\left(\frac{1}{n} \right) (\Sigma Y)^2 \right]}{n-1} \tag{13b}$$

where

PSI = present serviceability index

SV = slope variance

C = lineal feet of major cracking per 1,000 sq ft area

P = patching, sq ft per 1,000 sq ft area

RD = rut depth, in.

Y = difference in elevation, inches of two points 1 ft apart

Axle Load (kips)	Pavement Structural Number (SN)					
	1	2	3	4	5	6
2	.0001	.0001	.0001	.0000	.0000	.0000
4	.0005	.0005	.0004	.0003	.0003	.0002
6	.002	.002	.002	.001	.001	.001
8	.004	.006	.006	.004	.003	.003
10	.008	.013	.011	.009	.007	.006
12	.015	.024	.023	.018	.014	.013
14	.026	.041	.042	.033	.027	.024
16	.044	.065	.070	.057	.047	.043
18	.070	.097	.109	.092	.077	.070
20	.107	.141	.162	.141	.121	.110
22	.160	.198	.229	.207	.180	.166
24	.231	.273	.315	.292	.260	.242
26	.327	.370	.420	.401	.364	.342
28	.451	.493	.548	.634	.495	.470
30	.611	.648	.703	.695	.658	.633
32	.813	.843	.889	.887	.867	.834
34	1.06	1.08	1.11	1.11	1.09	1.08
36	1.38	1.38	1.38	1.38	1.38	1.38
38	1.75	1.73	1.69	1.68	1.70	1.73
40	2.21	2.16	2.06	2.03	2.06	2.14
42	2.76	2.67	2.49	2.43	2.61	2.61
44	3.41	3.27	2.99	2.88	3.00	3.16
46	4.18	3.98	3.58	3.40	3.55	3.79
48	6.08	4.80	4.26	3.98	4.17	4.49
50	6.12	6.76	6.03	4.64	4.86	5.28
52	7.33	6.87	6.93	6.38	6.63	6.17
54	8.72	8.14	6.96	6.22	6.47	7.15
56	10.3	9.6	8.1	7.2	7.4	8.2
58	12.1	11.3	9.4	8.2	8.4	9.4
60	14.2	13.1	10.9	9.4	9.6	10.7
62	16.5	15.3	12.6	10.7	10.8	12.1
64	19.1	17.6	14.6	12.2	12.2	13.7
66	22.1	20.3	16.6	13.8	13.7	15.4
68	25.3	23.3	18.9	16.6	15.4	17.2
70	29.0	26.6	21.5	17.6	17.2	19.2
72	33.0	30.3	24.4	19.8	19.2	21.3
74	37.5	34.4	27.6	22.2	21.3	23.6
76	42.5	38.9	31.1	24.8	23.7	26.1
78	48.0	43.9	35.0	27.8	26.2	28.8
80	54.0	49.4	39.2	30.9	29.0	31.7
82	60.6	55.4	43.9	34.4	32.0	34.8
84	67.8	61.9	49.0	38.2	35.3	38.1
86	75.7	69.1	54.5	42.3	38.8	41.7
88	84.3	76.9	60.6	46.8	42.6	45.6
90	93.7	85.4	67.1	51.7	46.8	49.7

Figure 24. AASHTO table of load equivalency factors for flexible pavements, tandem axles, and terminal serviceability index of 2.5 (AASHTO 1986)

n = number of readings

To apply the AASHTO design equation in this case it was necessary to use the same structural numbers (SN) as used to select the ESAL factors for each

Table 6
AASHTO Load Equivalency Factors

Item No.	Structural Number Sn	18-kip ESAL Factors			
		High Pressure		Low Pressure	
		Loaded	Unloaded	Loaded	Unloaded
4	1.10	2.19	0.126	2.07	0.126
5	1.22	2.19	0.131	2.08	0.131
6	1.14	2.19	0.126	2.07	0.126
7	1.56	2.22	0.145	2.10	0.145
8	2.13	2.25	0.169	2.14	0.169
9	2.00	2.25	0.167	2.13	0.167
10	1.70	2.22	0.154	2.11	0.154
11	1.70	2.22	0.154	2.11	0.154
12	1.41	2.22	0.143	2.10	0.143

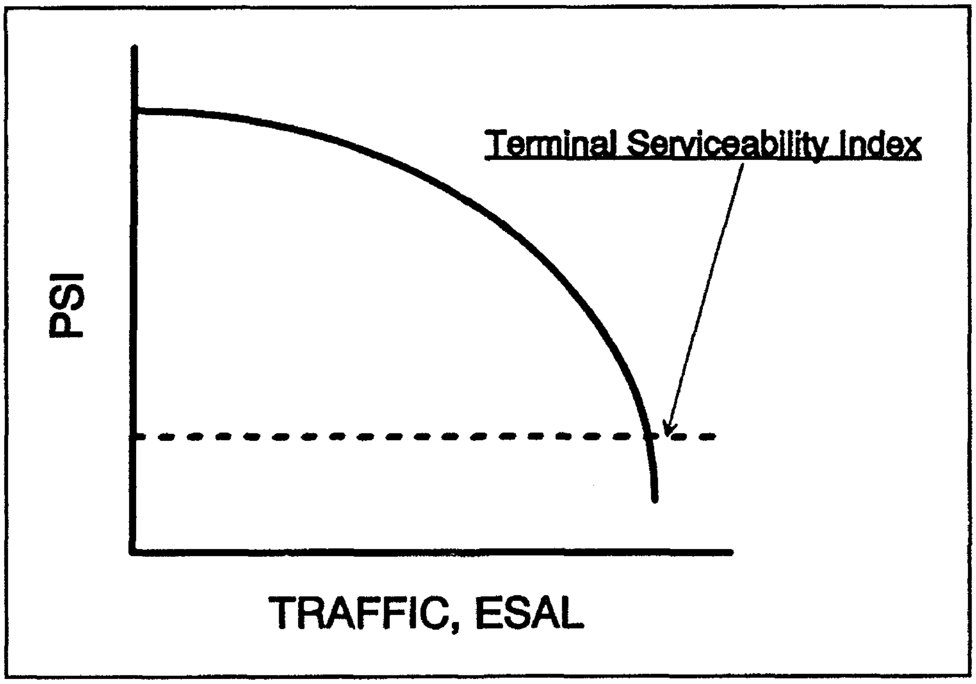

Figure 25. General relationship between PSI and applied traffic showing terminal serviceability index

test item. The AASHTO equation requires six input parameters as described above to calculate W18 as shown in Equation 4. The 1986 AASHTO design guide recommends a reliability of 50 percent with a variance of 0.35 for low volume roads. This value is also recommended in the FS STP design guide. Based on the available laboratory and field data and recommended values in the AASHTO design guide, a subgrade resilient modulus of 6,000 psi was used in calculating W18. A terminal PSI of 2.5 was the active failure criteria in the AASHTO analysis. These data were used to determine pavement life where failure was reached during traffic application. These comparisons are limited to the AC surfaced items 4, 5, and 6. These items represent the thinner surfaced AC test items which reached failure under a more orderly rate of progression. When failure was not reached, extrapolations of the data were used to estimate pavement life for test items The input data, predicted ESAL's (W18) and measured (or estimated) failure ESAL's are shown in Table 7. A plot of predicted W18 versus measured W18 for the AC surfaced test items is shown in Figure 26. Although the data does not give an exact 1 to 1 correlation, it does show that the test results do fall close to the predicted failure ESAL's especially where actual failure data were available. Most of the discrepancies in predicted and measured passes to failure are a result of the lack of actual failure data and PSI variations from spot failures in the road surface. The one major disadvantage of the AASHTO method is that tire pressure is a variable not accounted for in the equation.

Table 7
Results of AASHTO Analysis of AC Surfaced Items 4, 5, and 6

Item	Lane H or L	Structural Number, Sn	W18 from AASHTO	W18 from Data	F,SF,XF[1]
4	H	1.1	4,800	1,200	SF
4	L	1.1	4,800	8,000	F
5	H	1.22	8,100	4,000	F
5	L	1.22	8,100	10,000	XF
6	H	1.14	5,800	4,000	F
6	L	1.14	5,800	6,000	F

[1] F = failure; SF = spot failure; XF = extrapolated failure.

The estimated ESAL's were calculated with the following values common to all computations:

Reliability, R = 50 percent
Variance, So = 0.35
Subgrade Resilient
Modulus, Mr = 6,000 psi
Delta PSI = 2.5

Corps of Engineers CBR-based design procedure

The Corps of Engineers flexible pavement design equation was the second of the two empirical design models used in the analysis of the data from the AC-surfaced test items. The model was described in detail in Chapter 1 of

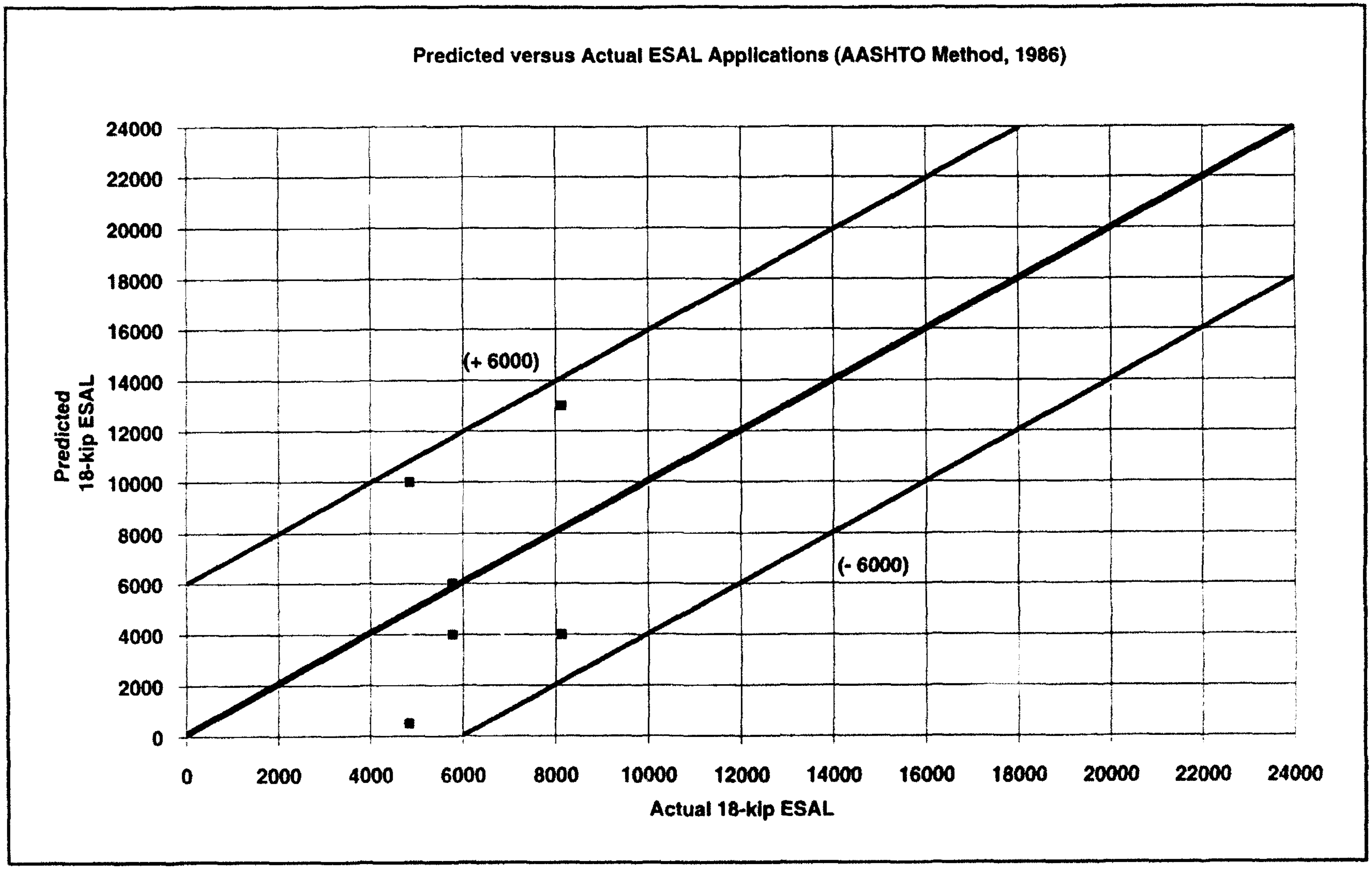

Figure 26. Predicted versus actual passes (AASHTO flexible pavement design procedure)

this report. It is a form of the CBR equation extended statistically with the results from tests on pavements with heavy gear multiple-wheel loads (Hammitt et al. 1971) shown as Equations 3a and 3b. A comparison of both CBR design equations to the original calibration data is shown in Figure 27.

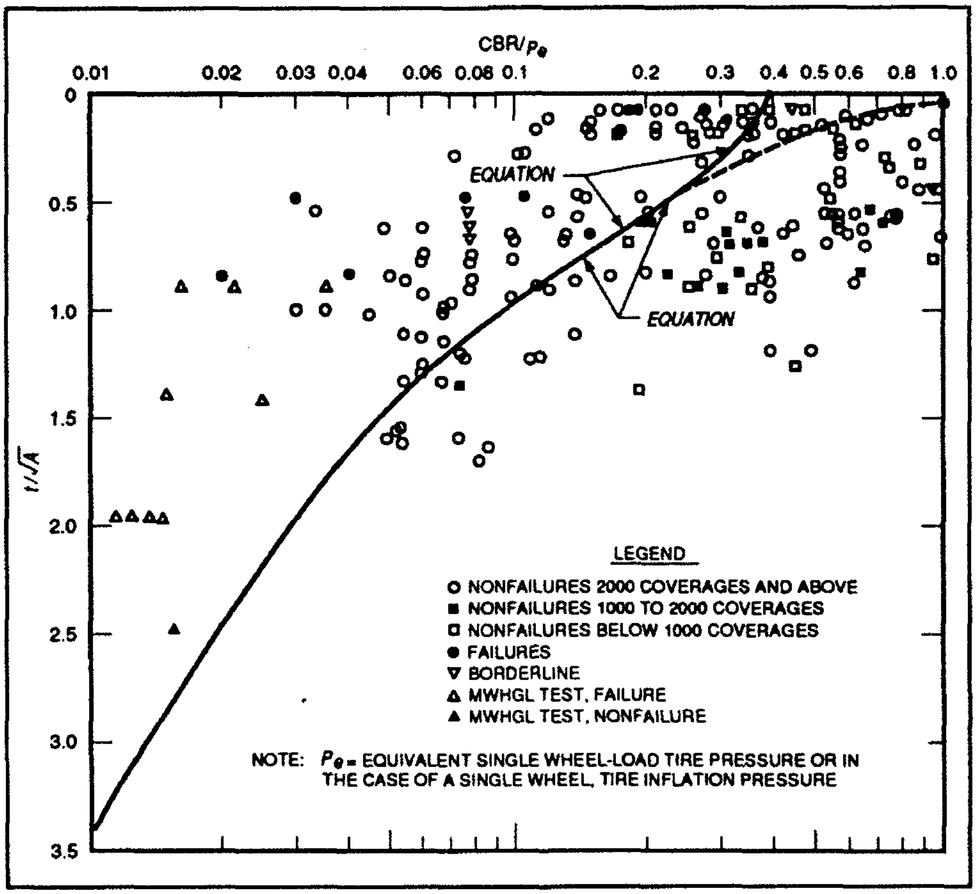

Figure 27. Comparison of original CBR data with Equations 2 and 3a (Does not include FS data.) (Hammitt et al. 1971)

$$\frac{T}{\sqrt{A_c}} = \alpha_i \left[-0.0481 - 1.1562 \left[\log \frac{CBR}{P} \right] - 0.6414 \left[\log \frac{CBR}{P} \right]^2 - 0.4370 \left[\log \frac{CBR}{P} \right]^3 \right] \qquad \text{(3a bis)}$$

$$\alpha_i = [0.23 \log(c) + 0.15] \qquad \text{(3b bis)}$$

where

T = pavement thickness, in.

A_c = tire contact area, sq in.

α_i = load repetition factor

CBR = CBR of the subgrade material

P = ESWL or SW tire contact pressure, psi

$ESWL$ = equivalent single wheel load, lb

C = coverages

In Equation 3a the p (tire pressure) term is a hypothetical value which is equal to ESWL/Ac and has no relation to the actual tire pressure except where a single wheel is considered for analysis. Another major difference between the two CBR equations is the inclusion of the load repetition factor α_i which is a thickness percentage value used to account for traffic repetitions. The α_i value is a function of the number of passes of a given vehicle as well as the number of wheels used in the calculation of the ESWL.

Equivalency relationships

A discussion of the pass equivalency concepts used in the Corps analysis is presented in the following section. As noted in the AASHTO analysis, a method of accounting for the effects of mixed traffic must be used to properly address any of the design models. The mixed loaded and unloaded traffic was converted to 18-kip ESAL's using the Corps equivalent operations factors (Brown and Ahlvin 1961). The traffic on both the high pressure and low pressure lanes was converted to passes of an 18-kip ESAL. Another important consideration in the Corps design procedure is the concept of coverages of a given vehicle. The 1971 Corps equation uses coverages as the standard unit for traffic applications. A coverage is defined as the inverse of the sum of the probabilities that a given point on a pavement will be traversed by some point on a tire (i.e. one coverage results when a given point on a pavement is traversed by any point on the tire). From TR 3-582 the pass to coverage ratio (P/C) for a standard 18-kip ESAL is 2.64, and the representative configuration of the Corps standard single axle is given in Figure 28. Therefore, it takes 2.64 passes of an 18-kip ESAL to give one coverage of the same using the Corps definition. The 18-kip ESAL loads were converted to ESWL values using the computer program developed by Gonzalez (1992). The program is an automated version of the procedures outlined in Taboza (1977). The ESWL values are needed as a direct input parameter in the Corps CBR equation. A plot of 18-kip ESAL coverages for both the high and low pressure lanes is given in Figure 29.

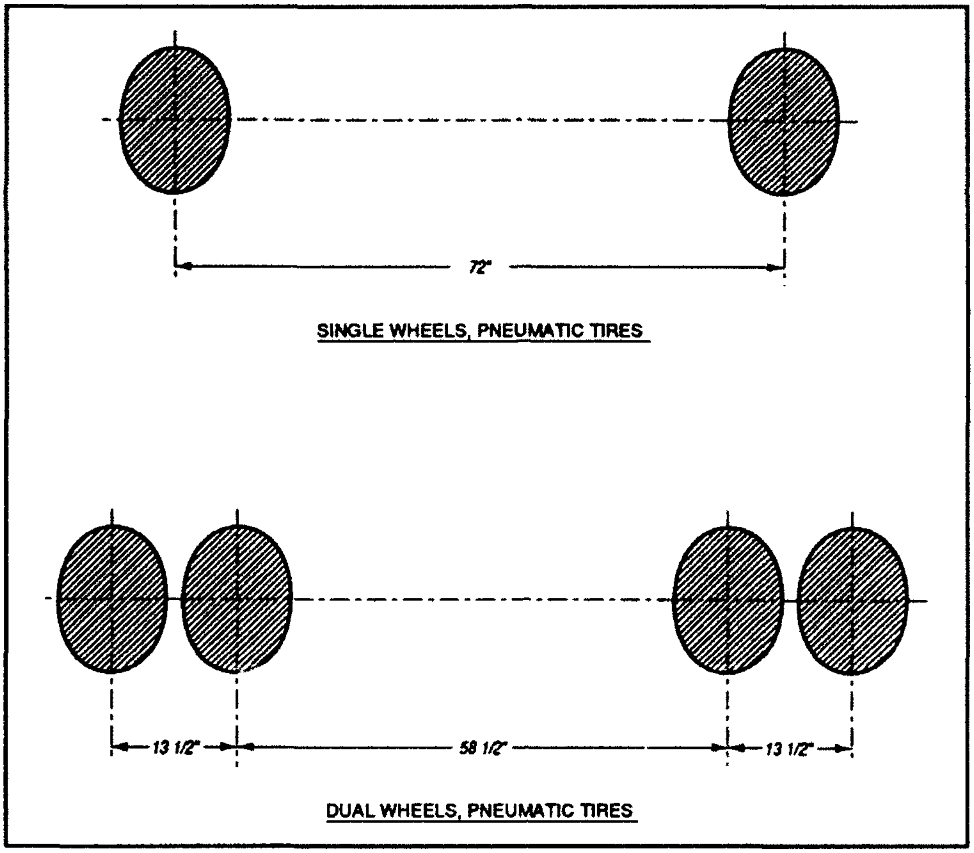

Figure 28. Standard axle wheel spacing for Corps flexible pavement design procedure

Calibration and verification of Corps flexible pavement design model

The major failure criterion for the Corps 1971 model is rut depth. Although rut depth is a major parameter in using the Corps 1971 equation, it is not explicitly accounted for in the equation. A failure criterion of a 1-in. rut depth was used in the following analysis. The Corps CBR equation was designed to calculate the thickness of each layer of a given pavement one at a time. In order to calculate pavement life from the structural pavement properties and traffic data, pavement layer thicknesses were converted to standard sections using the guidance presented in DA TM-5-822-5 (Headquarters, Department of the Army 1980). A standard asphalt thickness of 2 in. was used to determine equivalent base course thickness values. The 2-in. value corresponds to the minimum thickness recommended for a design index of 4 to 7 for a road or street. The AC in excess of 2 in. was converted to an equivalent base course thickness using an equivalency factor of 1.15 (Headquarters, Department of the Army 1980). The 2-in. AC thickness was then added to the equivalent base thickness to obtain a total section thickness for use in the analysis as shown in Equation 14:

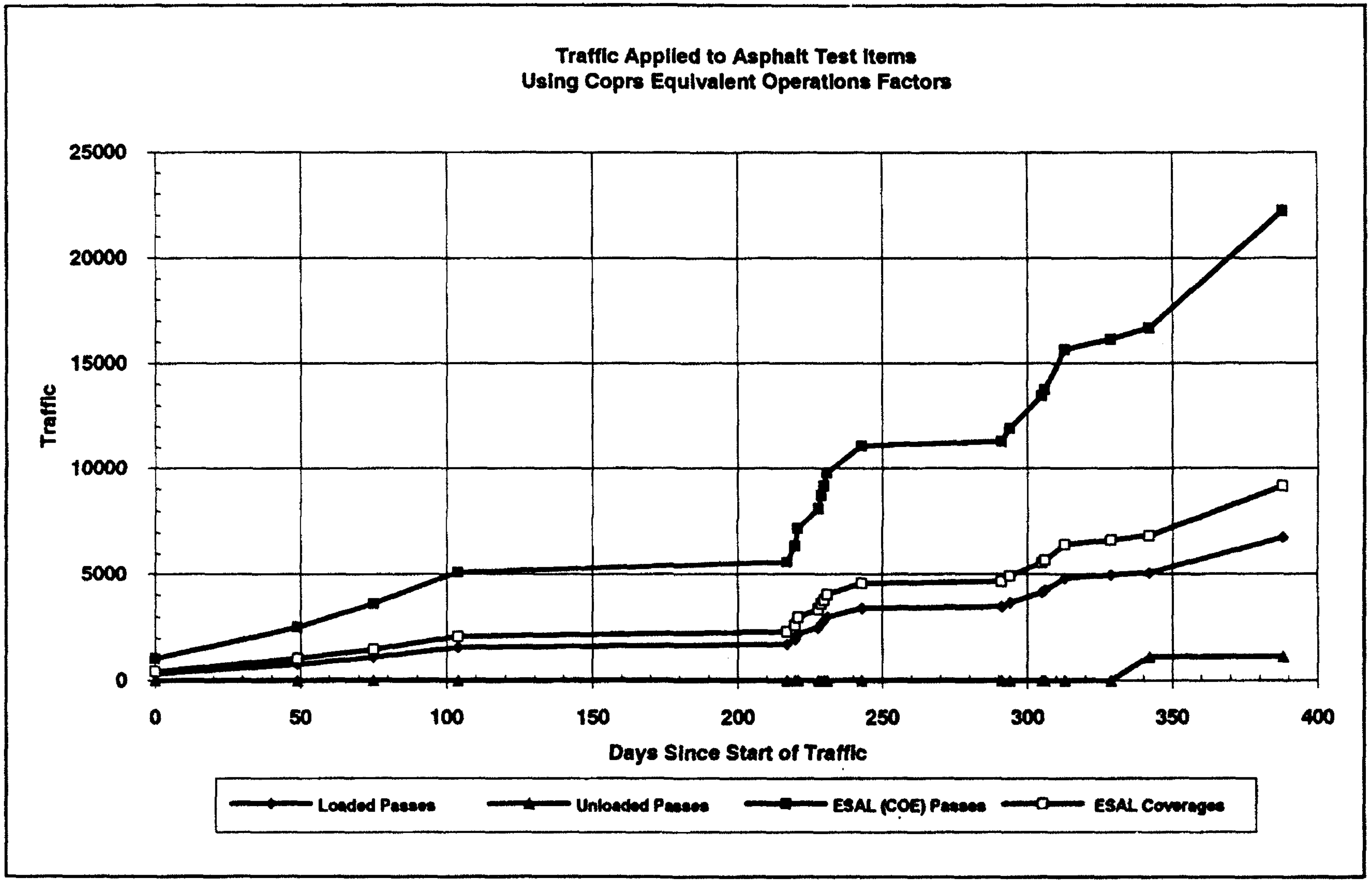

Figure 29. Traffic applied to asphalt test items using Corps equivalent operations factors

$$T_{EQ} = [(T_{ACC} - 2)(1.15)] + T_B + 2 \tag{14}$$

where

T_{EQ} = equivalent pavement thickness, in.

T_B = base course thickness, in.

T_{AC} = asphalt thickness, in.

Once the equivalent section thickness was determined, the other input parameters of ESWL, contact pressure, contact area, and subgrade CBR were obtained from the test data. During the initial portion of the analysis only the as-constructed CBR values were used, these values were different from the CBR values obtained from post-test pit excavations. A comparison plot of CBR/p versus T/(A) for the 1971 Corps equation and the CTI data with both as-constructed and rated CBR is shown in Figure 30. The rated CBR value is the average of the as-constructed and the post failure CBR values. From this plot it can be seen that the use of initial CBR values places the CTI data below the CBR equation in the nonfailure regime. It is also evident that the rated CBR values provide a much better agreement with the equation. These values were then input into the Corps 1971 equation to predict α_i. The predicted coverages were then computed using the α_i equation given above. The predicted passes were computed from the coverages using a pass to coverage ratio of 2.64, and compared to applied 18-kip ESAL coverages at failure as shown in Figure 31. The input parameters and predicted passes are given in Tables 8 and 9 for both lanes. The calculated pass levels are larger in 8 of the 17 cases than the measured or extrapolated passes to failure. Many of the small coverages at maximum rut were attributed to spot failures in the pavement which are very difficult to predict. In the items where actual failure data were available, both lanes of items 4, 5, 6 and the high pressure lane of item 10, the difference between the predicted and measured passes was smaller than in those where failure was not reached.

Mechanistic Analysis

A series of analyses were conducted on items 10 and 12 using a theoretically based mechanistic analysis procedure. The analysis was conducted only on items 10 and 12 since no other items were instrumented with MDD's which provide a major element in the verification of the results from the analysis methods. The analysis was based on the theory of layered elastic systems using a computer program (JULEA) developed by Dr. Jacob Uzan of the Technion at Haifa, Israel. The data from the MDD's installed in items 10 and 12 were used to calculate subgrade strain-pavement life relationships. These results were compared to the predicted values.

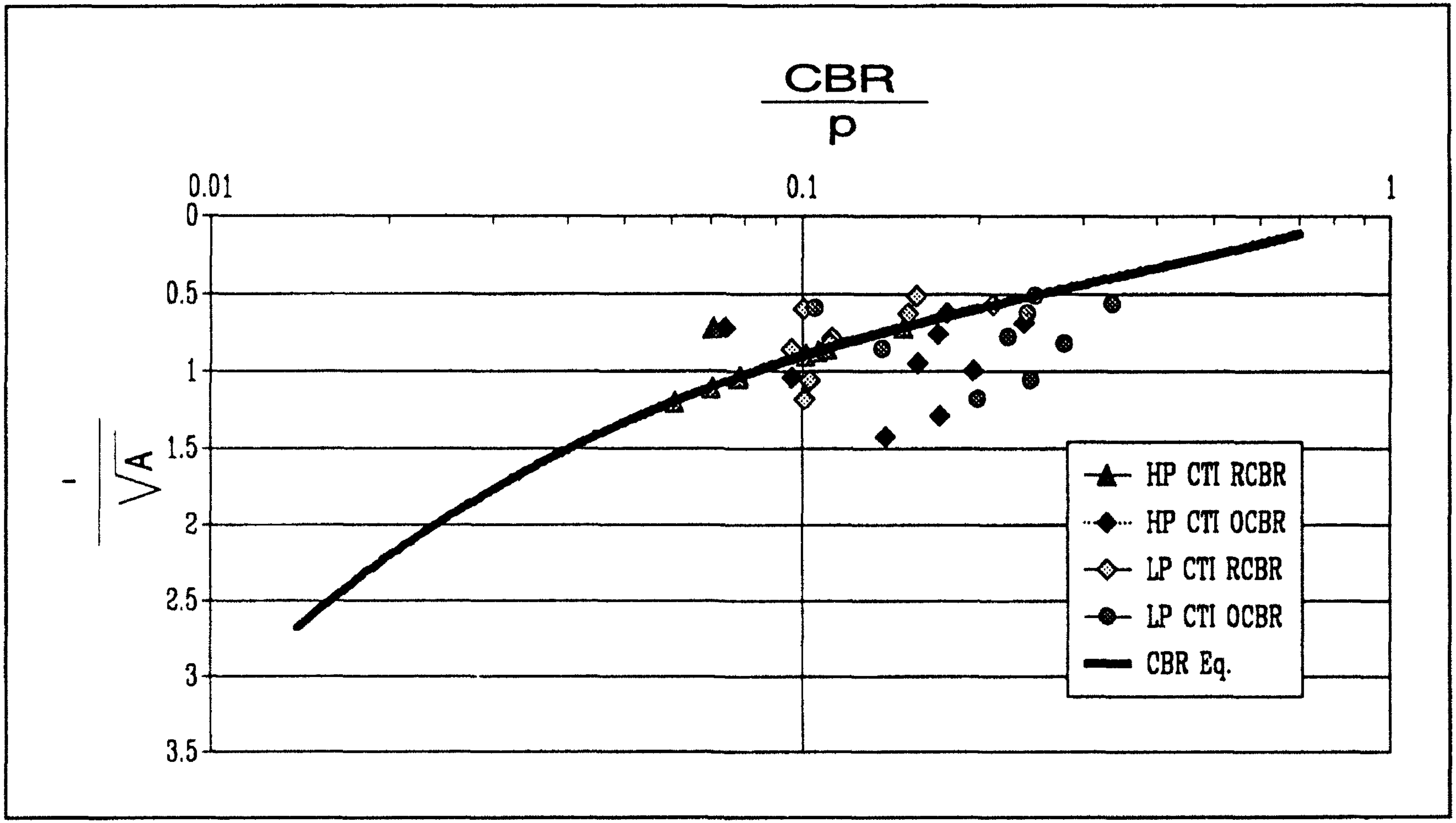

Figure 30. Comparison of CBR equation and CTI data where RCBR denotes rated CBR values, and OCBR denotes as-constructed CBR values

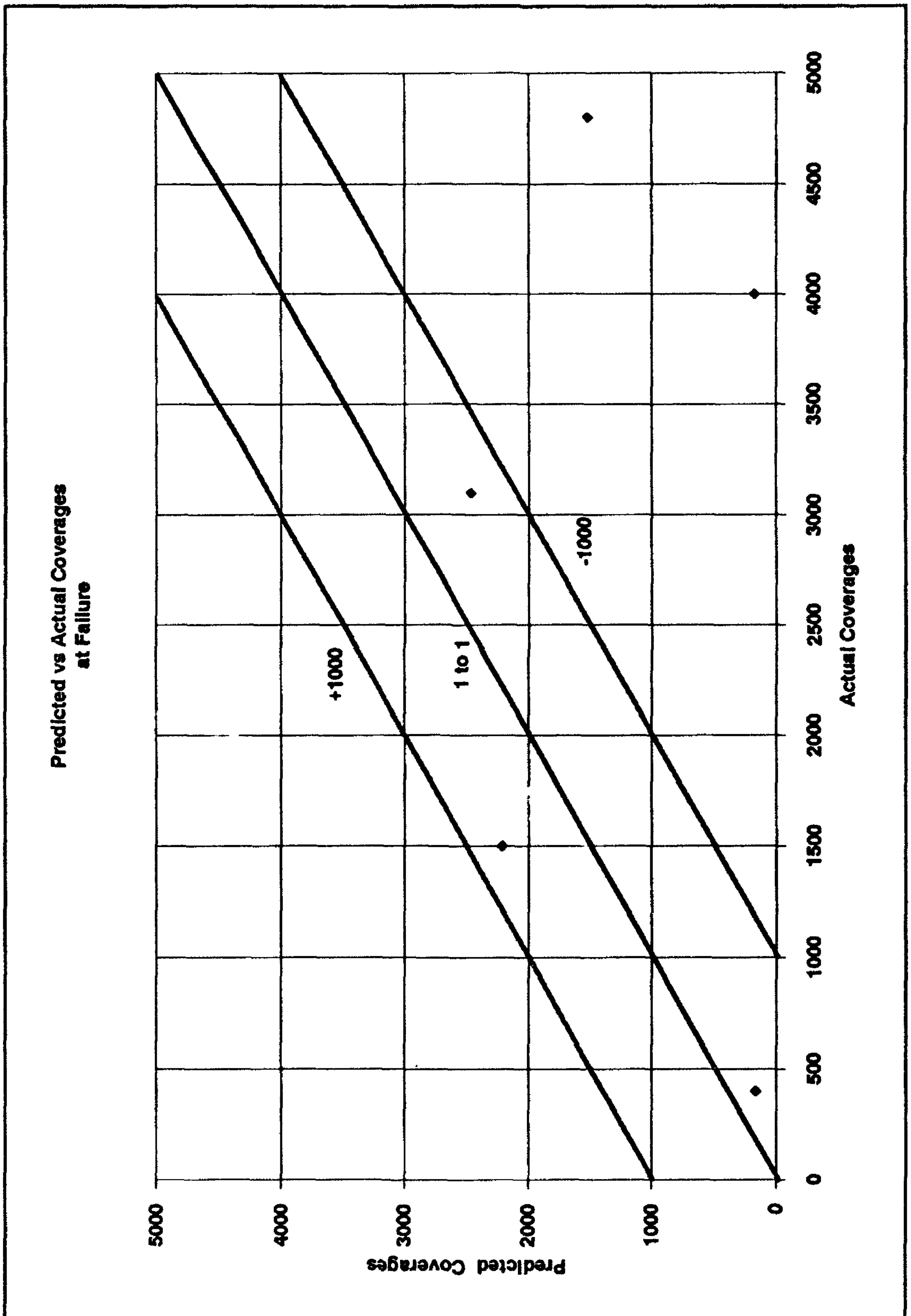

Figure 31. Predicted versus actual coverages at failure for the Corps flexible pavement design procedure

Table 8
Comparison of Failure Data and Predicted Passes from Corps

Item	Coverages at Max Rut	Max Rut, in.	Corps Eq. Coverages
4H	400	1.0	164
4L	1000	1.0	174
5H	2100	1.0	1810
5L	4800	1.0	1520
6H	1500	1.0	2210
6L	3100	1.0	2460
7H	3800	0.4	3390
7L	700	0.9	4570
8H	6000	0.8	92100
8L	8500	0.8	7.80E+07
9H	3500	0.6	38100
9L	4400	0.6	48000
10H	2400	1.0	3440
10L	5500	0.7	3890
11H	4800	0.4	1370
11L	8100	0.4	1560
12H	4100	0.5	325
12L	6800	0.5	358

Layered elastic analysis

Layered elastic analysis (LEA) is based on the following classical assumptions:

a. Each layer is homogeneous.

b. Each layer is isotropic.

c. Each layer has a finite thickness with the exception of the lowest layer which is considered infinite.

d. Material properties of each layer may be characterized by Young's modulus of elasticity and Poisson's ratio.

e. Each interface has rough conditions (full friction development).

f. Surface is free of horizontal loads.

These analyses are generally performed using one of the following solution methods:

a. One layer system: Boussinesq Method.

Table 9
Corps Flexible Pavement Design Method, Input Data, and Results

Item No.	Thickness, in. Asphalt	Agg.	Equiv.	Average Contact Area, sq in.	CBR of Subg.	Contact Pressure psi	ESWL, lb	Coverages ESAL
High Pressure Lanes								
4	2.8	3.0	6.0	68.2	7	94	6444	1.64e+02
5	2.7	5.8	8.6	68.2	6	104	7092	1.43e+03
6	2.3	5.5	7.8	68.2	8	102	6957	2.21e+03
7	5.2	0.0	5.7	68.2	14	92	6300	3.39e+03
8	5.0	6.3	11.8	68.2	8	116	7884	9.21e+04
9	4.7	5.5	10.6	68.2	11	111	7560	3.81e+05
10	4.3	3.6	8.2	68.2	8	102	6984	3.44e+03
11	5.7	0.0	6.3	68.2	10	94	6408	1.37e+03
12	4.7	0.0	5.1	68.2	10	91	6174	3.25e+02
Low Pressure Lanes								
4	2.8	3.0	6.0	99.9	7	66	6624	1.74e+02
5	2.7	5.8	8.6	99.9	6	73	7299	1.52e+03
6	2.3	5.5	7.8	99.9	8	71	7128	2.46e+03
7	5.2	0.0	5.7	99.9	14	65	6498	4.57e+03
8	5.0	6.3	11.8	99.9	8	80	8028	1.11e+05
9	4.7	5.5	10.6	99.9	11	78	7758	4.80e+05
10	4.3	3.6	8.2	99.9	8	72	7146	3.89e+03
11	5.7	0.0	6.3	99.9	10	66	6606	1.56e+03
12	4.7	0.0	5.1	99.9	10	64	6390	3.58e+02

b. Two layer system: Burmister Method.

c. Three layer system: Acum-Fox or Jones-Peattie Methods.

d. Multiple (greater than three) layer systems: Approximate solutions.

In general pavement problems are usually systems with three or more layers and require much more complex solution procedures than the above closed form methods. For this reason pavement layered elastic analysis is generally a computer oriented procedure.

The basic methodology of a mechanistic analysis is to compute stresses, strains, and deflections within the layers of a pavement system and then to

relate these values to performance and pavement life. The current Corps LEA design procedures predict structural deterioration by accounting for cumulative damage according to Miner's hypothesis. In these procedures, the damage factor is defined as the number of applied repetitions (n) of a given response parameter divided by the allowable repetitions (N) of the response parameter. The cumulative damage factor (CDF) for the parameter is the sum of the damage factors for the various values of the parameter. The CDF concept permits handling variations in material properties and loading/traffic conditions (Barker and Gonzalez 1991).

The structural deterioration of a flexible pavement is normally associated with cracking of the AC surface course and development of ruts in the wheel paths caused by strain repetitions due to a number of surface vehicular load applications. The asphalt strain failure criterion built into the current design procedure is represented in Equation 15:

$$
\begin{aligned}
C &= 10^{(a-b)} \\
a &= 2.68 - 5.0 \log(e_h) \\
b &= 2.665 \log(M_r)
\end{aligned}
\tag{15}
$$

where

c = allowable coverages

e_h = maximum asphalt horizontal strain, in./in.

M_r = modulus of elasticity of asphalt, psi

Rutting is considered to occur in the subgrade and is controlled by limiting the value of the vertical compressive strain in the top of the subgrade. The subgrade strain failure criteria are represented in Equation 16:

$$
\begin{aligned}
C &= 10000 \left[\frac{a}{e_v} \right]^{b} \\
a &= 0.000247 + 0.000245 \log(M_r) \\
b &= 0.0658\ M_r^{0.559}
\end{aligned}
\tag{16}
$$

where

c = allowable coverages

e_v = maximum subgrade vertical strain, in./in.

M_r = modulus of elasticity of subgrade, psi

These same criteria were used throughout the mechanistic portion of the analysis to relate strain to pavement life. The reference vehicle for strain calculations was a standard 18-kip dual-wheel single axle.

The ranges of elastic properties were determined from laboratory tests and backcalculation of FWD data described in Volume I. A range of values of Young's modulus and Poisson's ratio were established and used as the input material properties. The results of a JULEA based analysis are shown in Table 10. Subgrade vertical strain was the controlling criterion in all analysis

Table 10
Results of Layered Elastic Analysis for Items 10 and 12

Item	AC Thick. in.	Base Thick. in.	Modulus, E: AC psi	Modulus, E: Base psi	Modulus, E: Subg psi	Subg ϵ_v μ"/"	JULEA Predicted Coverages	High to Low % Diff.
10HP	4.3	3.6	25,0000	20,000	10,000	1018	8.30E+04	12
10LP	4.3	3.6	25,0000	20,000	10,000	1008	9.28E+04	
10HP	4.3	3.6	30,0000	50,000	10,000	802	1.24E+06	10
10LP	4.3	3.6	30,0000	50,000	10,000	795	1.37E+06	
10HP	4.3	3.6	40,0000	20,000	10,000	859	5.68E+05	13
10LP	4.3	3.6	40,0000	20,000	10,000	850	6.40E+05	
10HP	4.3	3.6	70,0000	50,000	10,000	621	2.24E+07	12
10LP	4.3	3.6	70,0000	50,000	10,000	615	2.50E+07	
12HP	4.7	0.0	25,0000	20,000	10,000	1114	2.99E+04	248
12LP	4.7	0.0	25,0000	20,000	10,000	998	1.04E+05	
12HP	4.7	0.0	30,0000	50,000	10,000	847	6.66E+05	303
12LP	4.7	0.0	30,0000	50,000	10,000	749	2.68E+06	
12HP	4.7	0.0	40,0000	20,000	10,000	860	5.61E+05	130
12LP	4.7	0.0	40,0000	20,000	10,000	799	1.29E+06	
12HP	4.7	0.0	70,0000	50,000	10,000	540	1.09E+08	123
12LP	4.7	0.0	70,0000	50,000	10,000	503	2.44E+08	

HP = High Pressure.
LP = Low Pressure.

cases, and is the basis for computing the allowable coverages from the analysis. The subgrade modulus values were kept constant at 10,000 psi while the AC surface modulus was varied from 200,000 psi to 700,000 psi for each structure and load case. In item 10 the estimated life of the pavement, in allowable coverages, showed an increase of 10 to 13 percent when contact

pressure was reduced from the high pressure setting to the low pressure setting. In item 12 the estimated pavement life increased by 123 to 248 percent when contact pressure was reduced from the high pressure setting to the low pressure setting. This difference in percent increase in pavement life between items 10 and 12 is attributed to the relative thinness of item 12, a 2-layer system, in relation to item 10, a 3-layer system.

Analysis of MDD data

Data from the MDD's installed in items 10 and 12 were used to determine subgrade strain under both high and low pressure configurations. These results and the tire pressures at the time of testing are shown in Table 11. Pavement life was computed with Equation 15 using the subgrade strain values obtained from the MDD data. These values showed large increase in pavement life from 100 psi tires to 40 psi tires and are shown in Table 12. The data also shows a decrease in measured strain as speed increases, which is due to the decrease in duration of load. This translates to an increase in estimated pavement life with increased speed. The differences in pavement life as a function of speed are only minimally sensitive to reductions in tire pressure.

Table 11
Pavement Response to High and Low Pressures on Items 10 and 12

Item	Tire Pressure psi	Speed MPH	Highest Maximum Deflection, mils			Average Strains, μ"/"	
			MDD1	MDD2	MDD3	Base	Subgrade
10HP	100	4.3	31.08	24.76	9.91	1,035	1,079
10HP	110	11.5	28.00	21.63	9.13	1,045	909
10HP	100	23.6	24.79	19.34	8.25	888	806
10LP	40	4.4	29.23	22.88	9.53	1,041	970
10LP	40	10.0	25.98	20.49	8.83	899	848
10LP	40	17.4	23.26	18.38	7.81	816	769
12HP	100	2.7	32.09	11.33	--	--	1,693
12HP	100	12.3	27.12	10.08	--	--	1,390
12HP	110	19.2	24.21	9.17	--	--	1,228
12LP	40	4.6	28.51	10.31	--	--	1,485
12LP	40	11.3	23.2	8.9	--	--	1,167
12LP	40	18.6	21.38	8.39	--	--	1,060

Table 12
Predicted Coverages from MDD Data

Item	Tire Pressure	Speed, MPH	Subgrade, ϵ_v, μ"/"	Predicted Coverages
10LP	40	4.4	970	143,375
10HP	110	4.3	1,079	42,901
10LP	40	10.0	848	657,457
10HP	110	11.5	909	299,272
10LP	40	17.4	769	1,990,867
10HP	110	23.6	806	1,168,998
12LP	40	4.6	1,485	1,151
12HP	110	2.7	1,693	261
12LP	40	11.3	1,167	17,648
12HP	110	12.3	1,390	2,434
12LP	40	18.6	1,060	52,467
12HP	110	19.2	1,228	9,908

Comparison of Design Models

In order to assess the strengths and weaknesses of each of the asphalt pavement design models comparisons were made between the three fully developed design methods, i.e.: AASHTO design guide, Corps of Engineers CBR design method, and layered elastic design method. Baseline material properties were used with given traffic and load characteristics. These values are given in Table 13.

Table 13
Input Data for Comparison of Design Methods

Basis of Comparison	Subgrade CBR	Base Course CBR/Thick.	Standard Load	Passes	AC Thickness
Thickness	7	35/NA	18-k ESAL	50,000	2 in.

The design methods were compared on the basis of design thickness as a function of tire pressure. Thickness designs are based on an AC surface layer 2 in. in thickness with a crushed limestone aggregate base course. The results of the thickness comparison are shown in Figure 32. No change is expected in design thickness with the AASHTO design method since it is independent of tire pressure. The Corps CBR procedure shows approximately a 1-in. reduction in required base thickness as tire pressure is reduced from 120 psi to 40 psi. The AASHTO procedure shows an average 1 in. additional

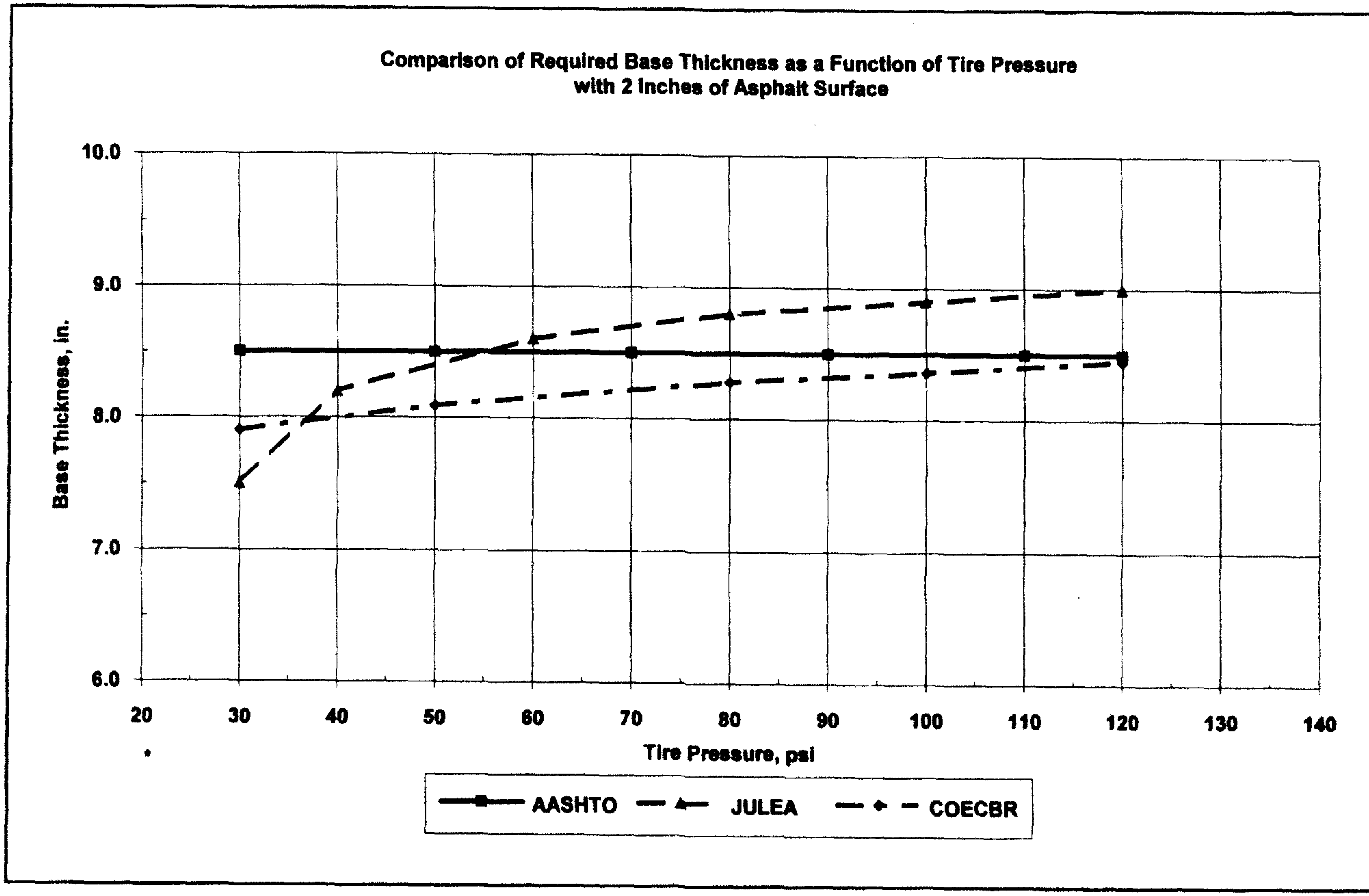

Figure 32. Comparison of Corps method, AASHTO method, and layered elastic design method

required thickness of base course over that required by the Corps procedure. This is most likely due to the extremely conservative nature of the AASHTO design procedure and the relatively low loads and traffic levels seen in this comparison.

4 Conclusions and Recommendations

Conclusions

An analysis of the data obtained during the application of traffic to the FS low-volume test road was used to adapt or develop design and serviceability models which account for the effects of variable tire pressures on low-volume aggregate surfaced and AC-surfaced roads. This chapter summarizes the results and findings of the analysis effort and provides recommendations on methods of accounting for variable tire pressure in design procedures and guidance documents. The design methods investigated are extremely sensitiv to the material property input data and therefore require the best available data when used for the design or analysis of low volume roads since these pavement types are at the lower end of the data regime from which the design methods were developed.

A 37 percent reduction in required thickness was predicted for the test case design values in Chapter 3 for an aggregate surfaced road where the tire pressures were reduced from 100 to 40 psi. A 10 to 12 percent reduction in required base thickness was predicted for the test case design values in Chapter 3 for an asphalt surfaced road where the tire pressures were reduced from 100 to 40 psi. However, these are representative values based on specific input properties and should be determined on a project by project basis for the greatest accuracy.

Recommendations

General

Although the amount of failure data available for many of the test items was very limited, a number of additional data points obtained under simulated field were added to the existing database on aggregate surface pavement performance. An updated set of design relationships were developed from this augmented database and were used to successfully demonstrate the beneficial effects of reducing tire pressure, and general guidance information was

obtained for the use of three flexible pavement design methods with variable tire pressures.

Aggregate surfaces

The analysis of the data from the aggregate-surfaced test items provided an opportunity to verify/modify the Corps of Engineers 1978 aggregate surfaced design equation developed by Barber, Odom, and Patrick (1978), which is the design method in STP 1.02, the FS computer program for design of aggregate-surfaced roads. The equation was updated using the most reliable data from the CTI test road, and the new form of Equation 12, denoted as T92, is recommended for use as the current thickness design equation as shown below.

$$\log(t) = (0.2959)\,\frac{P_k^{0.2016}\; t_p^{0.2481}\; R^{0.0747}}{RD^{0.2128}\; C_1^{0.2414}\; C_2^{0.0596}} \qquad \text{(12 bis)}$$

where

t = aggregate depth, in.

P_k = ESWL, kips

t_p = tire pressure, psi

R = passes of ESWL

RD = rut depth, in.

C_1 = CBR of aggregate surface

C_2 = CBR of subgrade

Also, the original thickness design equation (Barber, Odom, and Patrick 1978) was based on an algebraic manipulation of a multiple linear regression, whereas the new equation, T92, is a direct application of a multiple linear regression with thickness as the dependent variable. When calculations are to be performed to determine parameters other than thickness, it is recommended that new equations be derived from a statistical regression about the variable of interest. The use of equivalency relationships should be standardized and carefully documented when using the aggregate surfaced design equation.

Asphalt concrete surfaces

The analysis of the data from the asphalt-surfaced test items provided an opportunity to verify/modify a number of current flexible pavement design methods. The analysis included both empirical and mechanistic methods.

The two empirical methods investigated were the AASHTO guide for the design of flexible pavements and the Corps of Engineers CBR-based flexible pavement design procedure. The mechanistic method investigated was the Corps of Engineers procedure based on layered elastic theory. The basic findings indicate that the AASHTO design guide provides an acceptable method for the design of low volume asphalt pavements. However, the AASHTO method does not have the ability to account for reduced tire pressures. The Corps of Engineers CBR based flexible pavement design procedure provides a good procedure for the design of low volume asphalt pavements as well as the ability to account for reduced tire pressure. If an empirical procedure is required for the design of asphalt pavements in an area where CTI equipped vehicles will be operating, the Corps design procedure is recommended as the preferred empirical design method. The use of the Corps method will allow designers to take full advantage of the reductions in design thickness caused by reduced tire pressures. When determining equivalent traffic, careful attention should be paid to the type of equivalency relationship used, since the relationships are tied to a given design method. For example, the AASHTO method for determining 18-kip ESAL should not be used with the Corps design procedure.

The mechanistic method of pavement analysis investigated was based on layered elastic theory. The LEA provided an opportunity to study the effects of tire pressure on pavement life and design thickness with a fully functional design procedure not based on empirical equations. From the comparisons performed with the AASHTO and Corps procedure, it was shown that the LEA procedure provides an acceptable alternative to the more traditional empirical methods of designing low volume road and pavements. The LEA procedure provides for directly accounting for reduced tire pressures as well as handling mixed traffic and environmental changes. For any future use of the LEA design procedures in the area of low volume road design, a more specific set of failure criteria should be developed. Once specific criteria are developed, the LEA design procedure can efficiently address design life considerations as well as structural adequacy. The material properties needed to design a pavement using LEA are not determined using standard characterization tests, but are not difficult to obtain when the proper test equipment is used. Relationships for equating elastic properties to more conventional pavement material properties are available but should be used only when direct measurement of these properties is not possible.

Future research

It is recommended that future tests be performed to further investigate the performance of pavements to variable tire pressure under the following conditions:

a. No mixed traffic be applied. This will remove the need for equivalency concepts in the analysis.

b. No maintenance be performed during traffic application unless baseline geometric and material property tests are performed before reapplication of traffic.

c. Future test sections need to be constructed strictly for the purpose of providing data for a mechanistic analysis, thereby enabling a much more rigorous analysis to be performed.

References

Ahlvin, Richard G. (1991). "Origin of developments for structural design of pavements," Technical Report GL-91-26, U.S. Army Engineer Waterways Experiment Station, Vicksburg, MS.

American Association of State Highway and Transportation Officials (AASHTO). (1986). Guide for design of pavement structures, Washington, DC.

ARE Inc.-Engineering Consultants. (1989). "Aggregate surfacing design guide and computer program," Unpublished Synthesis Report, USDA Forest Service, Washington, DC.

__________ . (1990). "Aggregate surfacing design guide," Final Report, USDA Forest Service, Washington, DC.

Barber, V. C., Odom, E. C., and Patrick, R. W. (1978). "The deterioration and reliability of pavements," Technical Report S-78-8, U.S. Army Engineer Waterways Experiment Station, Vicksburg, MS.

Barker, Walter R., and Gonzalez, Carlos R. (1991). "Pavement design by elastic layer theory," Proceedings of the ASCE Conference on Aircraft/ Pavement Interaction, Kansas City, MO.

Brown, D. N., and Ahlvin, R. G. (1961). "Revised design of roads and streets," Technical Report 3-582, U.S. Army Engineer Waterways Experiment Station, Vicksburg, MS.

Headquarters, Department of the Army. (1990). "Design of aggregate surfaced roads and airfields," Technical Manual TM-5-822-12, Washington, DC.

__________ . (1980). "Engineering and design, flexible pavements for roads streets, walks, and open storage areas," Technical Manual TM 5-822-5, Washington, DC.

__________ . (1968). "Planning and design of roads, airbases, and heliports in the theater of operations," Technical Manual TM 5-530, Washington, DC.

Gonzalez, Carlos R. (1992). "A computer program for the calculation of the equivalent single-wheel load factor," Miscellaneous Paper GL-92-18, U.S. Army Engineer Waterways Experiment Station, Vicksburg, MS.

Grau, Robert. (1993). "Effects of variable tire pressure on road surfacings: Volume 1, Design, construction, and behavior under traffic," in preparation, U.S. Army Engineer Waterways Experiment Station, Vicksburg, MS.

Grau, Robert. (1990). "Effects of variable tire pressure on road surfacings," Miscellaneous Paper GL-90-21, U.S. Army Engineer Waterways Experiment Station, Vicksburg, MS.

Hammitt, G. M. II. (1970). "Thickness requirements for unsurfaced roads and airfields," Technical Report S-70-5, U.S. Army Engineer Waterways Experiment Station, Vicksburg, MS.

Hammitt, G. M. II, Hutchinson, R. L., Rice, J. L., Thompson, O. O., and Brown, D. N. (1971). "Multiple-wheel heavy gear load pavement tests, Volume IV: analysis of behavior under traffic," TR S-71-17, U.S. Army Engineer Waterways Experiment Station, Vicksburg, MS.

Porter, O. J. (1938). "The preparation of subgrades," Proceedings, Highway Research Board, Pt. II, p. 324.

Porter, O. J. (1942). "Foundation for flexible pavements" Proceedings, Highway Research Board, p. 100

Scullion, Tom, Bush A. J. III, and Kenis, W. J. (1990). "Use of the multi-depth deflectometer to evaluate tire pressure effects in flexible pavements," Proceedings of the Third International Conference on Bearing Capacity of Roads and Airfields.

Taboza, P. A. (1977). "Procedures for development of CBR design curves," Instructional Report S-77-1, U.S. Army Engineer Waterways Experiment Station, Vicksburg, MS.

USDA Forest Service. (1974). "Interim guide for thickness design of flexible pavement structures," FSH 7709.11, Chapter 50, Region 6 Supplement No. 20, Portland, OR.

Webster, Steve L., Grau, Richard H., Williams, Thomas P. (1992). "Description and application of dual mass dynamic cone penetrometer," Instructional Report GL-92-3, U.S. Army Engineer Waterways Experiment Station, Vicksburg, MS.

Yoder, E. J. and Witczak, M. W. (1975). "Principles of pavement design," Wiley-Interscience, John Wiley and Sons.

Appendix A
Test Results

Gravel-Surfaced Facility Data (Barber) 1978							
Point No.	Rut, in.	ESWL, lb	Tp, psi	T, in.	Surface CBR	Subgrade CBR2	Rep
1	0.5	4.68	100	4.5	81	19.5	920
2	1	4.68	100	4.5	81	19.5	3,240
3	1.2	4.68	100	1.5	81	19.5	6,760
4	0.6	4.8	70	4.5	69	18.5	3,400
5	0.7	4.8	70	4.5	69	18.5	6,480
6	0.2	5.44	40	4.5	64	18	1,080
7	0.5	5.44	40	4.5	64	18	3,800
8	0.6	5.44	40	4.5	64	18	6,800
9	0.2	5.92	20	4.5	50	17.5	1,160
10	0.45	5.92	20	4.5	50	17.5	2,660
11	0.5	5.92	20	4.5	50	17.5	6,120
12	0.5	5.44	40	10	29	21	1,880
13	0.6	5.44	40	10	29	21	2,940
14	0.4	5.92	20	4.5	55	9	800
15	0.6	5.92	20	4.5	55	9	4,000
16	0.8	5.92	20	4.5	55	9	6,400
17	0.2	8	20	4.5	44	7	120
18	0.8	8	20	4.5	44	7	800
19	1.6	8	20	4.5	44	7	4,000
20	2.5	25	100	12	5.3	4.7	17
21	3.2	25	100	12	5.3	4.7	30
22	2	25	100	12	8	5.3	17
23	2.2	25	100	12	8	5.3	30
24	2.4	25	100	12	8	5.3	43
25	2	25	100	12	7	4.9	17
26	2.4	25	100	12	7	4.9	30
27	2.7	25	100	12	7	4.9	43
28	2.75	15	150	6	9	3.2	91
29	3.84	15	150	6	9	3.2	108
30	4.91	15	150	6	9	3.2	133
31	1.16	15	150	12	7.5	3.5	41
32	1.52	15	150	12	7.5	3.5	66
33	2.02	15	150	12	7.5	3.5	108
34	2.47	15	150	12	7.5	3.5	133
35	3	15	150	12	7.5	3.5	158
36	3.6	15	150	12	7.5	3.5	199
37	1.04	15	150	18	9	3.7	41
38	1.12	15	150	18	9	3.7	66
39	1.47	15	150	18	9	3.7	108
40	1.75	15	150	18	9	3.7	133
41	1.88	15	150	18	9	3.7	199
							(Sheet 1 of 7)

Point No.	Rut, in.	ESWL, lb	Tp, psi	T, in.	Surface CBR	Subgrade CBR2	Rep
42	2.92	15	150	18	9	3.7	291
43	3.1	15	150	18	9	3.7	332
44	3.48	15	150	18	9	3.7	365
45	1.55	15	150	24	7.6	3.2	41
46	1.13	15	150	24	7.6	3.2	66
47	1.52	15	150	24	7.6	3.2	108
48	1.53	15	150	24	7.6	3.2	133
49	1.82	15	150	24	7.6	3.2	199
50	2.57	15	150	24	7.6	3.2	291
51	2.53	15	150	24	7.6	3.2	332
52	2.97	15	150	24	7.6	3.2	365
53	1.85	25	115	12	7.5	3	29
54	3.7	25	115	12	7.5	3	109
55	1.79	25	115	18	8.2	3.3	29
56	1.96	25	115	18	8.2	3.3	57
57	2.86	25	115	18	8.2	3.3	109
58	3.86	25	115	18	8.2	3.3	144
59	1.39	25	115	24	9	3.1	29
60	1.21	25	115	24	9	3.1	57
61	1.5	25	115	24	9	3.1	109
62	2.31	25	115	24	9	3.1	144
63	3.37	25	115	24	9	3.1	333
64	1	40	80	12	11	3.7	11
65	2.29	40	80	12	11	3.7	56
66	3.61	40	80	12	11	3.7	90
67	1.72	40	80	18	9.3	3.4	187
68	2.22	40	80	18	9.3	3.4	262
69	2.84	40	80	18	9.3	3.4	337
70	3.75	40	80	18	9.3	3.4	449
71	1.66	40	80	6	9	3.7	8
72	3.47	40	80	6	9	3.7	17
73	1.16	40	80	12	11	2.9	17
74	1.85	40	80	12	11	2.9	55
75	2.44	40	80	12	11	2.9	76
76	3.54	40	80	12	11	2.9	98
77	0.82	40	80	18	9.7	3.6	17
78	0.94	40	80	18	9.7	3.6	55
79	1.57	40	80	18	9.7	3.6	76
80	1.81	40	80	18	9.7	3.6	98
81	2.1	40	80	18	9.7	3.6	157
82	2.82	40	80	18	9.7	3.6	212
83	2.78	40	80	18	9.7	3.6	233
84	2.91	40	80	18	9.7	3.6	254

(Sheet 2 of 7)

Point No.	Rut, in.	ESWL, lb	Tp, psi	T, in.	Surface CBR	Subgrade CBR2	Rep
85	3.25	40	80	18	9.7	3.6	297
86	1.22	40	80	24	9.7	4.3	212
87	1.19	40	80	24	9.7	4.3	233
88	1.16	40	80	24	9.7	4.3	254
89	1.32	40	80	24	9.7	4.3	297
90	1.62	40	80	24	9.7	4.3	424
91	1.72	40	80	24	9.7	4.3	636
92	2.25	40	80	24	9.7	4.3	848
93	2.57	40	80	24	9.7	4.3	1,060
94	2.66	15	165	6	11	4.4	8
95	3.36	15	165	6	11	4.4	16
96	1.33	15	165	12	10	3.8	8
97	1.48	15	165	12	10	3.8	16
98	0.59	15	165	18	13	4.5	8
99	0.85	15	165	18	13	4.5	16
100	1.16	15	165	18	13	4.5	56
101	1.56	15	165	18	13	4.5	80
102	2.41	15	165	18	13	4.5	127
103	2.97	15	165	18	13	4.5	159
104	3.25	15	165	18	13	4.5	175
105	0.65	15	165	24	11	4.1	8
106	0.97	15	165	24	11	4.1	16
107	1.35	15	165	24	11	4.1	56
108	1.97	15	165	24	11	4.1	80
109	2.56	15	165	24	11	4.1	127
110	2.72	15	165	24	11	4.1	159
111	3.07	15	165	24	11	4.1	175
112	2.63	40	120	6	13	3.5	13
113	3.9	40	120	6	13	3.5	17
114	1.65	40	120	12	12	4	17
115	3.78	40	120	12	12	4	76
116	1.31	40	120	18	11	4.7	17
117	2.28	40	120	18	11	4.7	76
118	2.47	40	120	18	11	4.7	127
119	2.81	40	120	18	11	4.7	170
120	3.2	40	120	18	11	4.7	212
121	0.88	40	120	24	11	5.1	17
122	1.53	40	120	24	11	5.1	76
123	1.65	40	120	24	11	5.1	127
124	2.04	40	120	24	11	5.1	170
125	2.57	40	120	24	11	5.1	212
126	2.66	40	120	24	11	5.1	254

(Sheet 3 of 7)

Point No.	Rut, in.	ESWL, lb	Tp, psi	T, in.	Surface CBR	Subgrade CBR2	Rep
127	2.75	40	120	24	11	5.1	297
128	3.25	40	120	24	11	5.1	339
129	0.78	26.6	120	12	10	4.3	5
130	1.88	26.6	120	12	10	4.3	49
131	1.97	26.6	120	12	10	4.3	82
132	2.5	26.6	120	12	10	4.3	114
133	3.38	26.6	120	12	10	4.3	147
134	1.31	26.6	120	18	9.9	4.1	49
135	1.57	26.6	120	18	9.9	4.1	114
136	1.97	26.6	120	18	9.9	4.1	147
137	2.28	26.6	120	18	9.9	4.1	196
138	2.29	26.6	120	18	9.9	4.1	245
139	2.47	26.6	120	18	9.9	4.1	293
140	2.78	26.6	120	18	9.9	4.1	342
141	3.16	26.6	120	18	9.9	4.1	391
142	1.57	26.6	120	24	11	4.4	49
143	1.66	26.6	120	24	11	4.4	114
144	1.94	26.6	120	24	11	4.4	147
145	2.07	26.6	120	24	11	4.4	196
146	1.94	26.6	120	24	11	4.4	245
147	2	26.6	120	24	11	4.4	293
148	2.16	26.6	120	24	11	4.4	342
149	2.72	26.6	120	24	11	4.4	391
150	2.5	26.6	120	24	11	4.4	440
151	3.52	26.6	120	24	11	4.4	473
152	2.38	25	125	15	18	2.7	431
153	2.63	25	125	15	18	2.7	545
154	2.94	25	125	15	18	2.7	689
155	3.56	25	125	15	18	2.7	861
156	4.06	25	125	15	18	2.7	941
157	2.19	25	125	18	17	2.9	712
158	2.69	25	125	18	17	2.9	861
159	2.81	25	125	18	17	2.9	941
160	2.65	25	125	18	17	2.9	1,091
161	2.85	25	125	18	17	2.9	1,538
162	3	25	125	18	17	2.9	1,722
163	3.25	25	125	18	17	2.9	1,866
164	4	25	125	18	17	2.9	2,003
165	1.69	25	125	21	17	2.6	1,866
166	1.63	25	125	21	17	2.6	2,003
167	1.56	25	125	21	17	2.6	2,153
168	1.66	25	125	21	17	2.6	2,296
169	1.69	25	125	21	17	2.6	2,440

(Sheet 4 of 7)

Point No.	Rut, in.	ESWL, lb	Tp, psi	T, in.	Surface CBR	Subgrade CBR2	Rep
170	1.75	25	125	21	17	2.6	2,583
171	1.81	25	125	21	17	2.6	2,727
172	1.88	25	125	21	17	2.6	2,870
173	2.06	40	125	15	15	2.4	42
174	2.48	40	125	15	15	2.4	85
175	2.83	40	125	15	15	2.4	127
176	3.93	40	125	15	15	2.4	170
177	2.12	40	125	18	15	2.9	42
178	2.43	40	125	18	15	2.9	85
179	3	40	125	18	15	2.9	127
180	3.31	40	125	18	15	2.9	170
181	3.62	40	125	18	15	2.9	233
182	1.87	40	125	21	14	2.6	233
183	2.13	40	125	21	14	2.6	276
184	2.13	40	125	21	14	2.6	318
185	2.38	40	125	21	14	2.6	424
186	2.44	40	125	21	14	2.6	530
187	2.69	40	125	21	14	2.6	636
188	2.81	40	125	21	14	2.6	742
189	2.81	40	125	21	14	2.6	848
190	2.87	40	125	21	14	2.6	954
191	2.87	40	125	21	14	2.6	1,060
192	2.94	40	125	21	14	2.6	1,166
193	3	40	125	21	14	2.6	1,272
194	3.25	40	125	21	14	2.6	1,484
195	3.13	40	125	9	12	2.4	11
196	5.62	40	125	9	12	2.4	19
197	2.13	40	125	12	13	2.3	11
198	2.62	40	125	12	13	2.3	19
199	3.25	40	125	12	13	2.3	37
200	1.75	40	125	15	16	2.2	37
201	2.75	40	125	15	16	2.2	75
202	3.06	40	125	15	16	2.2	105
203	3.31	40	125	15	16	2.2	116
204	2.06	40	125	18	14	2.9	116
205	2.13	40	125	18	14	2.9	150
206	2.25	40	125	18	14	2.9	187
207	2.25	40	125	18	14	2.9	224
208	2.5	40	125	18	14	2.9	262
209	2.62	40	125	18	14	2.9	299
210	2.75	40	125	18	14	2.9	337
211	2.81	40	125	18	14	2.9	374

(Sheet 5 of 7)

Point No.	Rut, in.	ESWL, lb	Tp, psi	T, in.	Surface CBR	Subgrade CBR2	Rep
212	2.87	40	125	18	14	2.9	411
213	2.94	40	125	18	14	2.9	486
214	3.08	40	125	18	14	2.9	524
215	3.2	40	125	18	14	2.9	561
216	3.08	40	125	18	14	2.9	598
217	3.31	40	125	18	14	2.9	636
218	3.5	40	125	18	14	2.9	673
219	1.75	40	125	21	17	2.4	673
220	1.78	40	125	21	17	2.4	748
221	1.88	40	125	21	17	2.4	860
222	1.98	40	125	21	17	2.4	935
223	2.08	40	125	21	17	2.4	1,047
224	2.09	40	125	21	17	2.4	1,103
225	2.13	40	125	21	17	2.4	1,167
226	2.22	40	125	21	17	2.4	1,290
227	2.31	40	125	21	17	2.4	1,403
228	1.3	25	123	12	10	4.3	57
229	2.2	25	123	12	10	4.3	115
230	2.6	25	123	12	10	4.3	172
231	3.3	25	123	12	10	4.3	230
232	3.8	25	123	12	10	4.3	287
233	1.5	25	123	12	10	3.9	57
234	2.1	25	123	12	10	3.9	115
235	2.4	25	123	12	10	3.9	172
236	3.2	25	123	12	10	3.9	230
237	4.5	25	123	12	10	3.9	287
238	2.3	25	123	12	10	3.8	115
239	2.7	25	123	12	10	3.8	172
240	3.4	25	123	12	10	3.8	230
241	4.1	25	123	12	10	3.8	287
242	0.11	10	100	8	100	6.2	35
243	0.19	10	100	8	100	6.2	35
244	0.21	10	100	8	100	6.2	353
245	0.23	10	100	8	100	6.2	706
246	0.29	10	100	8	100	6.2	3,530
247	0.7	10	100	8	100	6.2	6,001
248	0.12	10	100	11	132	6.2	35
249	0.15	10	100	11	132	6.2	141
250	0.2	10	100	11	132	6.2	353
251	0.2	10	100	11	132	6.2	706
252	0.19	10	100	11	132	6.2	1,765
253	0.2	10	100	11	132	6.2	3,530
254	0.3	10	100	11	132	6.2	6,001

(Sheet 6 of 7)

USDA FS CTI Aggregate-Surfaced Test Results							
Point No.	Rut	Pk	Tp	T, in.	CBR1	CBR2	Rep
1	0.5	5.53	100	2.5	35	15	28
2	0.92	5.53	100	2.5	35	15	2,800
3	3.21	5.53	100	2.5	35	15	3,172
4	0.54	5.99	39	2.5	35	15	34
5	0.94	5.99	39	2.5	35	15	1,920
6	1.33	5.99	39	2.5	35	15	3,286
7	4.21	5.99	39	2.5	35	15	3,672
8	0.77	6.215	100	5.75	32	12	27
9	1.38	6.215	100	5.75	32	12	2,589
10	0.67	6.762	39	5.75	32	12	32
11	1.5	6.762	39	5.75	32	12	2,991
12	0.88	7.129	100	7.5	32	17	25
13	1.77	7.129	100	7.5	32	17	1,046
14	2.04	7.129	100	7.5	32	17	2,385
15	3.17	7.129	100	7.5	32	17	2,717
16	0.83	7.603	39	7.5	32	17	31
17	2.11	7.603	39	7.5	32	17	1,266
18	2.38	7.603	39	7.5	32	17	2,764
19	3.04	7.603	39	7.5	32	17	3,115
							(Sheet 7 of 7)

REPORT DOCUMENTATION PAGE

Form Approved
OMB No. 0704-0188

1. AGENCY USE ONLY *(Leave blank)*

2. REPORT DATE
August 1993

3. REPORT TYPE AND DATES COVERED
Final report

4. TITLE AND SUBTITLE
Effects of Variable Tire Pressure on Road Surfacings
Volume II: Analysis of Test Results

5. FUNDING NUMBERS

6. AUTHOR(S)
Donald M. Smith

7. PERFORMING ORGANIZATION NAME(S) AND ADDRESS(ES)
U.S. Army Engineer Waterways Experiment Station
Geotechnical Laboratory
3909 Halls Ferry Road, Vicksburg, MS 39180-6199

8. PERFORMING ORGANIZATION REPORT NUMBER
Technical Report GL-93-20

9. SPONSORING/MONITORING AGENCY NAME(S) AND ADDRESS(ES)
U.S. Department of Agriculture Forest Service
Technology and Development Center
444 East Bonita Avenue, San Dimas, CA 91773

10. SPONSORING/MONITORING AGENCY REPORT NUMBER

11. SUPPLEMENTARY NOTES
Available from National Technical Information Service, 5285 Port Royal Road, Springfield, VA 22161.

12a. DISTRIBUTION/AVAILABILITY STATEMENT
Approved for public release; distribution is unlimited.

12b. DISTRIBUTION CODE

13. ABSTRACT *(Maximum 200 words)*

This study was to determine the effects of variable tire pressure on road surfacings. A specially designed test road was constructed and subjected to both loaded and unloaded 18-wheeled log trucks operating in two distinct traffic lanes. The traffic was applied with the trucks operating at low and high tire pressures. This report provides an analytical summary of the types of test results obtained from the traffic applied to the test road and to use those test results to analyze, adapt, and develop design models which account for variable tire pressures on low-volume aggregate surfaced and asphalt-concrete surfaced roads.

Although the amount of failure data available for many of the test items was very limited, a number of additional data points obtained under simulated field were added to the existing database on aggregate surface pavement performance. An updated set of design relationships were developed from this augmented database and were used to successfully demonstrate the beneficial effects of reducing tire pressure, and general guidance information was obtained for the use of three flexible pavement design methods with variable tire pressures.

14. SUBJECT TERMS

Aggregate	Native material	Traffic tests
Asphalt concrete	Pavement analysis	Variable tire pressures
Central tire inflation	Pavement design	
Maintenance	Road surfacings	

15. NUMBER OF PAGES
84

16. PRICE CODE

17. SECURITY CLASSIFICATION OF REPORT	18. SECURITY CLASSIFICATION OF THIS PAGE	19. SECURITY CLASSIFICATION OF ABSTRACT	20. LIMITATION OF ABSTRACT
UNCLASSIFIED	UNCLASSIFIED		